

Robust Zero-Field Skyrmion Formation in FeGe Epitaxial Thin Films

Fengyuan Yang

The Ohio State University

Acknowledgements:

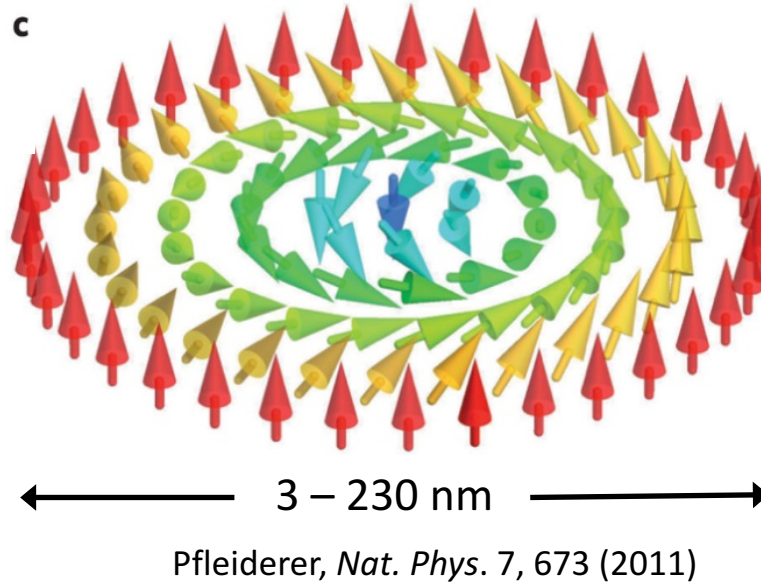
James Gallagher, Keng-Yuan Meng, Jack Brangham, Hailong Wang, Bryan Esser, Vidya Praveen Bhallamudi, David McComb, P. Chris Hammel

U.S. Department of Energy (DOE), Office of Science, Grant No. DE-SC0001304
Center for Emergent Materials, NSF-funded MRSEC, Grant No. DMR-1420451

Outline

- Magnetic skyrmions and topological Hall effect
- Growth of FeGe thin films by UHV off-axis sputtering
- Structural properties of FeGe films
 - X-ray diffraction
 - Scanning transmission electron microscopy (STEM)
- Hall effect measurement of FeGe films
 - Extraction of topological Hall effect
- Robust skyrmion phase
 - Highest topological Hall resistivity observed to date
 - High remanent topological Hall resistivity at $H = 0$
- Summary

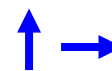
Magnetic Skyrmions



$$H = -J(\mathbf{S}_i \cdot \mathbf{S}_j) + \mathbf{D}_{ij} \cdot (\mathbf{S}_i \times \mathbf{S}_j)$$

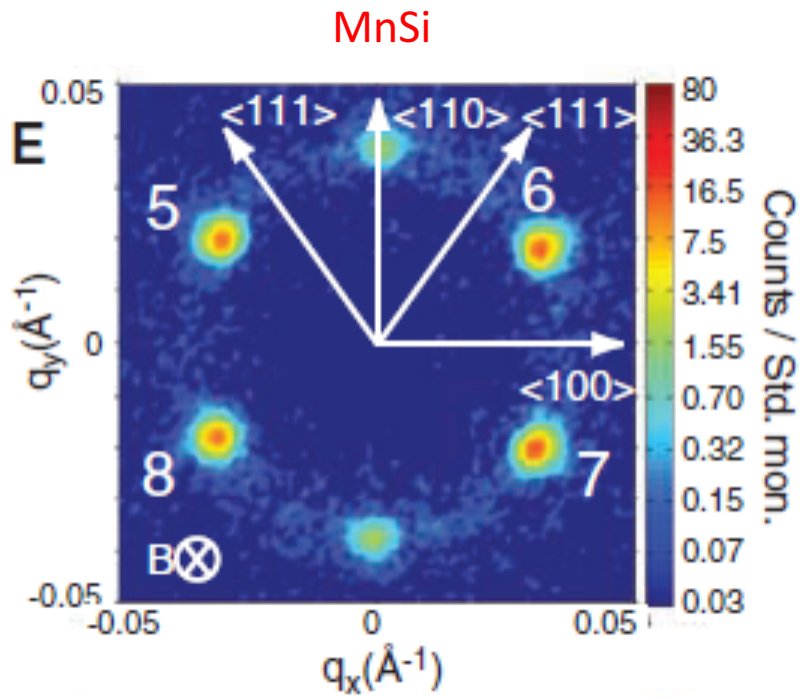


Heisenberg
Exchange

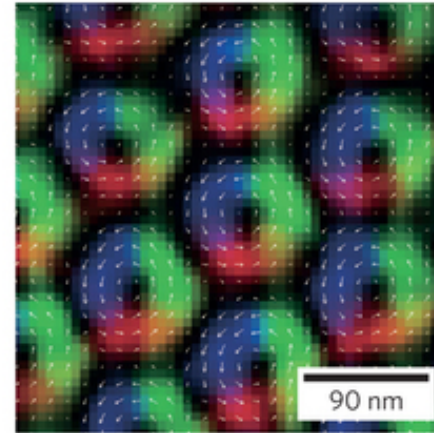


Dzyaloshinskii-Moriya
Interaction (DMI)

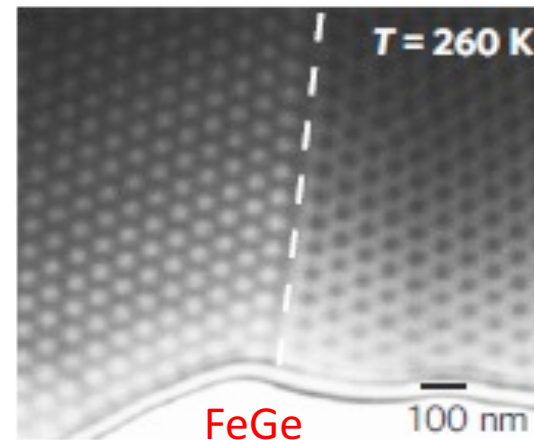
Magnetic Skyrmions



Mühlbauer, et al. *Science* 323, 915 (2009)

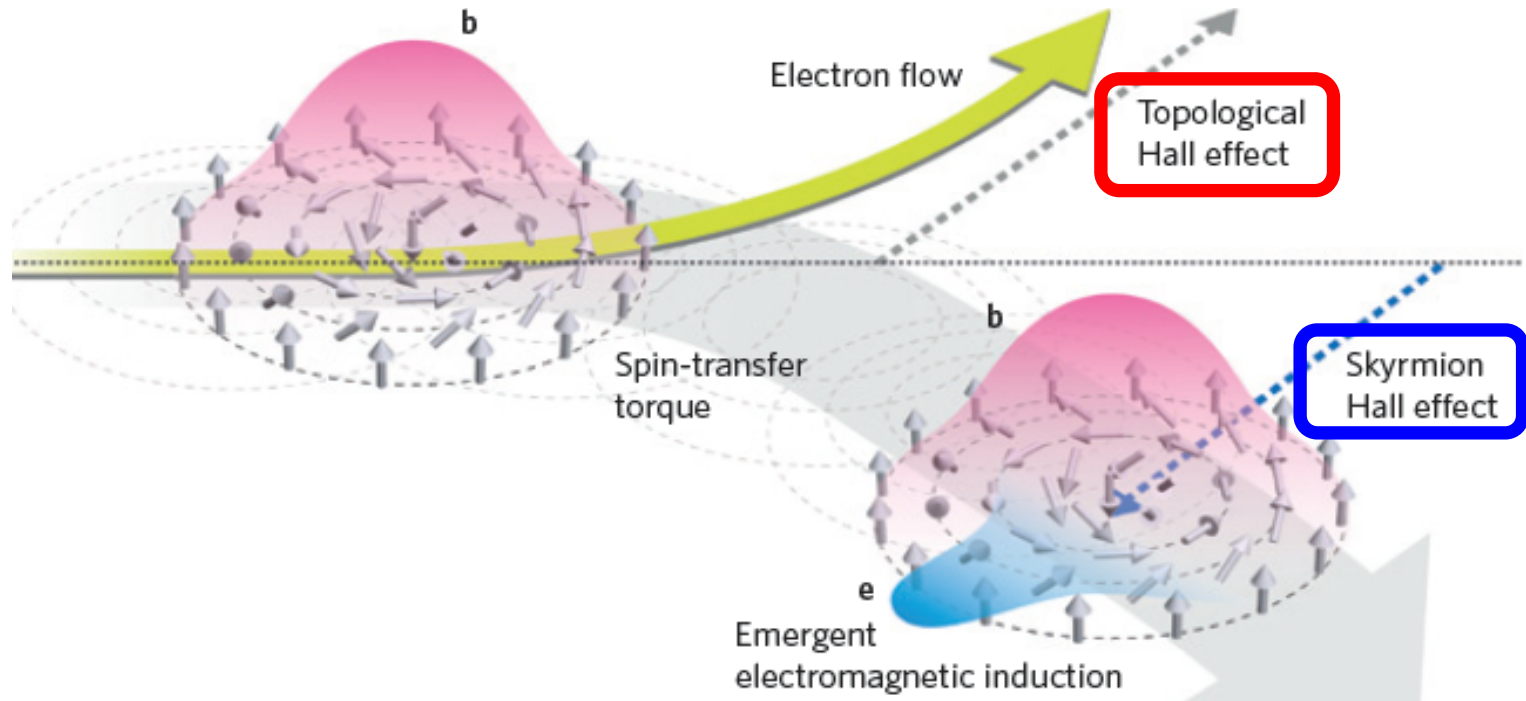


Fert, et al. *Nat. Nano.* 8, 152 (2013)



Yu, et al. *Nat. Mater.* 10, 106 (2011)

Current-driven skyrmion motion



- Skyrmions can be manipulated by very low electric current
- Potential for low energy memory/logic application

Nagaosa & Tokura, *Nat. Nano.* 8, 899 (2013)

Topological Hall effect in skyrmion films

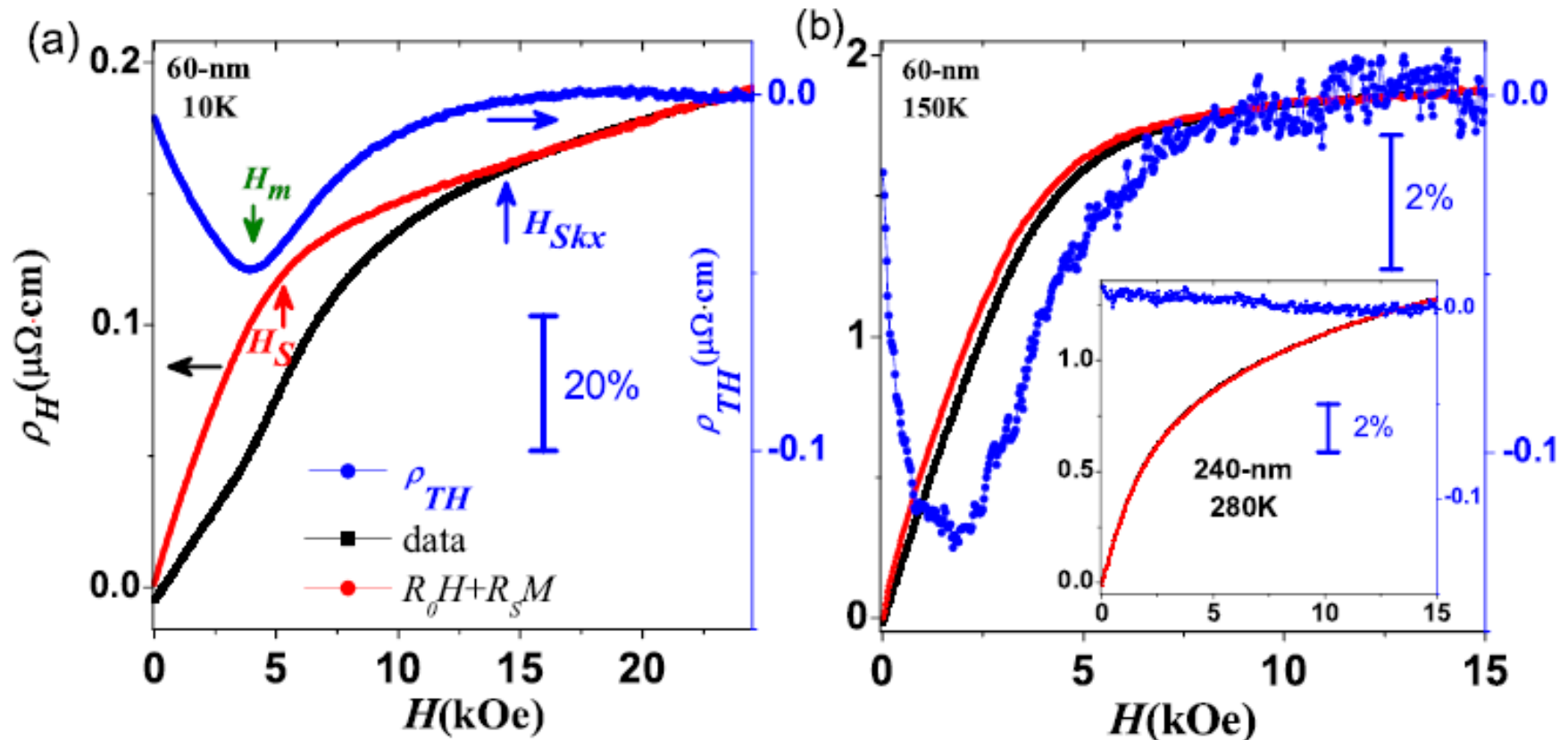
PRL 108, 267201 (2012)

PHYSICAL REVIEW LETTERS

week ending
29 JUNE 2012

Extended Skyrmion Phase in Epitaxial FeGe(111) Thin Films

S. X. Huang* and C. L. Chien†



Huang & Chien, *Phys. Rev. Lett.* 108, 267201 (2012)

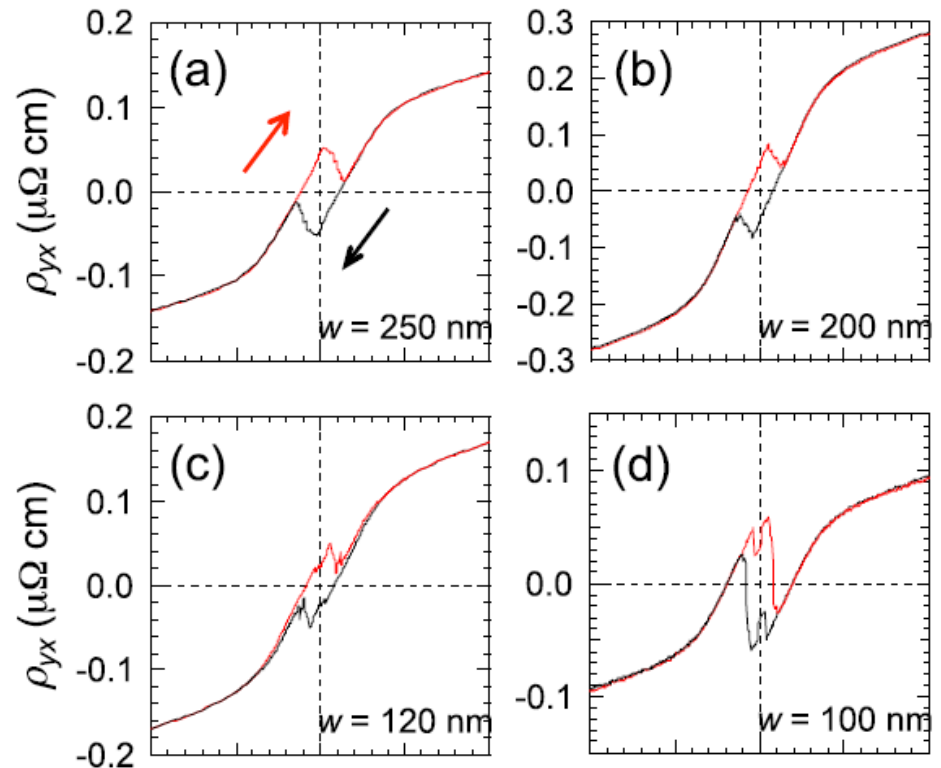
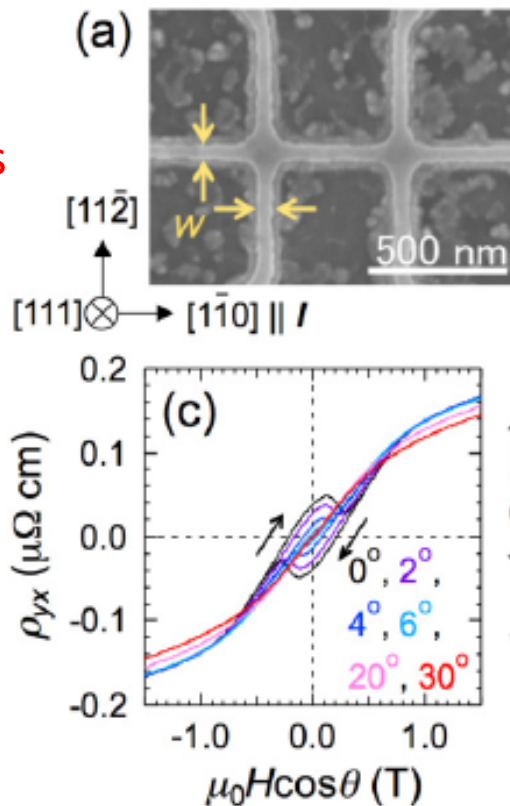
Topological Hall effect in skyrmion films

PHYSICAL REVIEW B **91**, 041122(R) (2015)

Discretized topological Hall effect emerging from skyrmions in constricted geometry

N. Kanazawa,¹ M. Kubota,^{2,3,*} A. Tsukazaki,⁴ Y. Kozuka,¹ K. S. Takahashi,² M. Kawasaki,^{1,2}
M. Ichikawa,¹ F. Kagawa,² and Y. Tokura^{1,2}

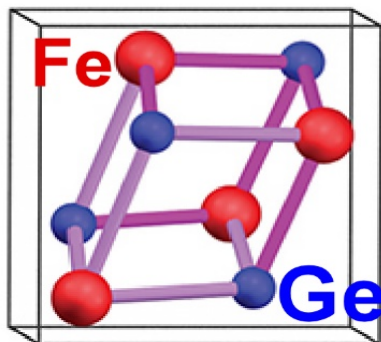
FeGe
Epi-films



B20 skyrmion materials

Technologically important if B20-phase skyrmions exist

- At zero magnetic field
- At room temperature.



B20 cubic lattice
noncentrosymmetric

Nagaosa & Tokura, *Nat. Nano.* 8, 899 (2013)

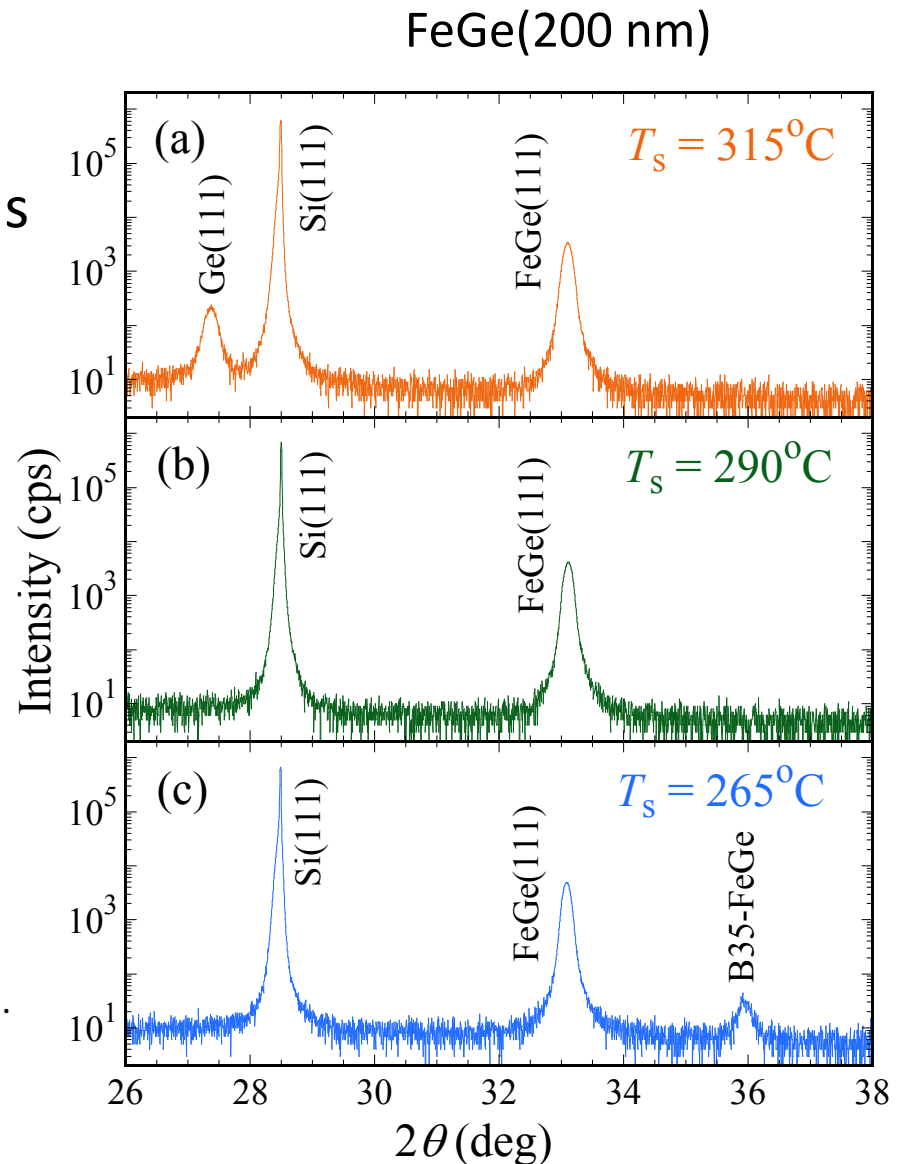
Material		T_N (K)	λ (nm)
MnSi	Bulk	30	18
	Epitaxial thin film	45	8.5
Mn _{1-x} Fe _x Si	$x = 0.06$	16.5	12.5
	$x = 0.08$	10.6	11
	$x = 0.10$	6.8	10
Fe _{1-x} Co _x Si	$x = 0.10$	11	43
	$x = 0.5$	36	90
	$x = 0.6$	24	174
	$x = 0.7$	7	230
MnGe	$T = 20$ K	170	3
	$T = 100$ K	-	3.4
	$T = 150$ K	-	5.5
Mn _{1-x} Fe _x Ge	$x = 0.35$	150	4.7
	$x = 0.5$	185	14.5
	$x = 0.7$	210	77
	$x = 0.84$	220	220
FeGe	Bulk	278	70
Cu ₂ OSeO ₃	Bulk	59	62
	Thinned plate	-	50

X-Ray Diffraction of FeGe films

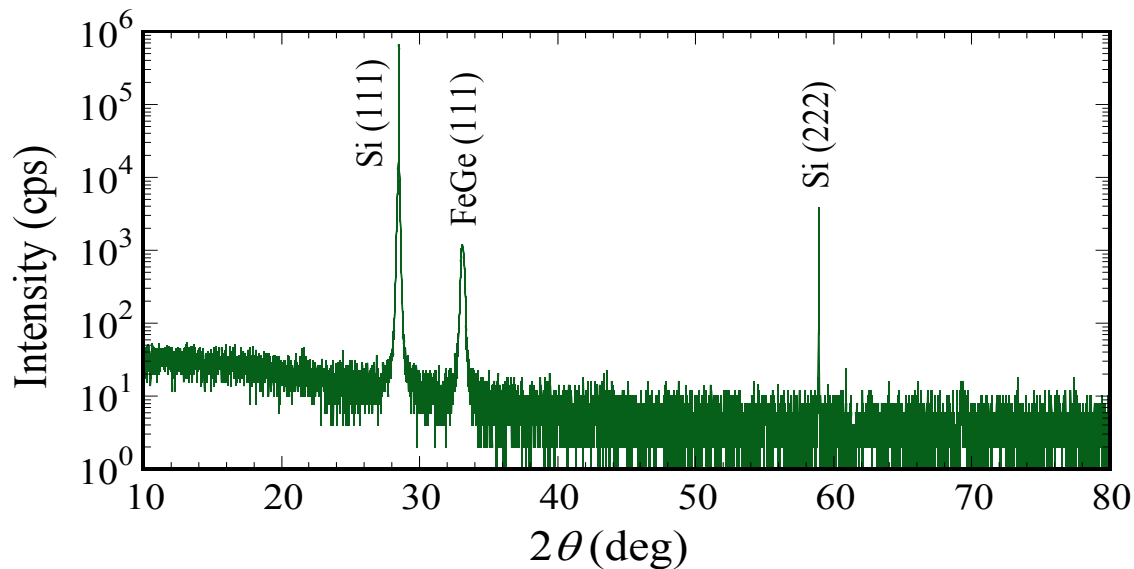
Deposition of FeGe epitaxial films

- UHV off-axis sputtering
- Base pressure: 10^{-11} Torr
- Gas: 5 mTorr Argon
- Growth rate: 0.67 nm/min
- FeGe film quality sensitive to substrate temperature

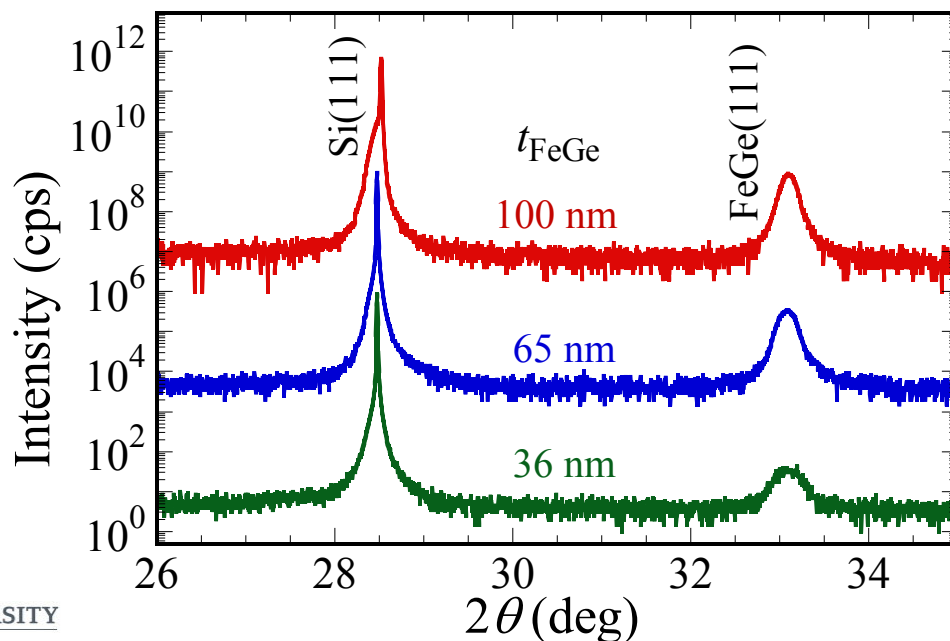
J. C. Gallagher, *et al.* Phys. Rev. Lett. 118, 027201 (2017).



X-Ray Diffraction of FeGe films

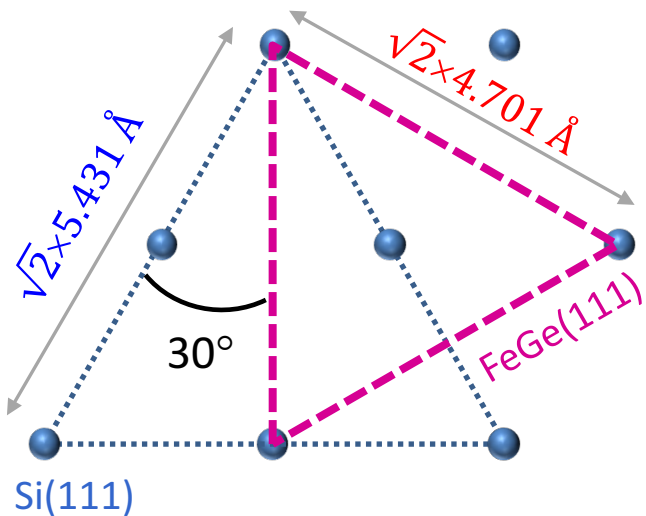
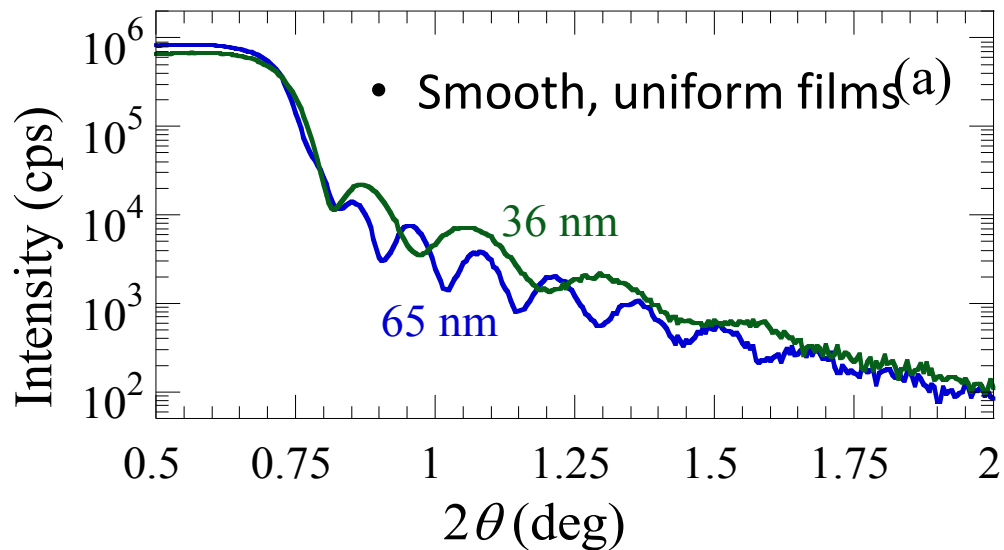
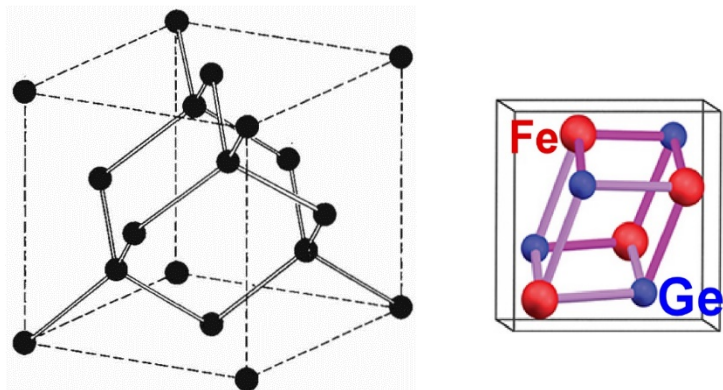


FeGe(200 nm)

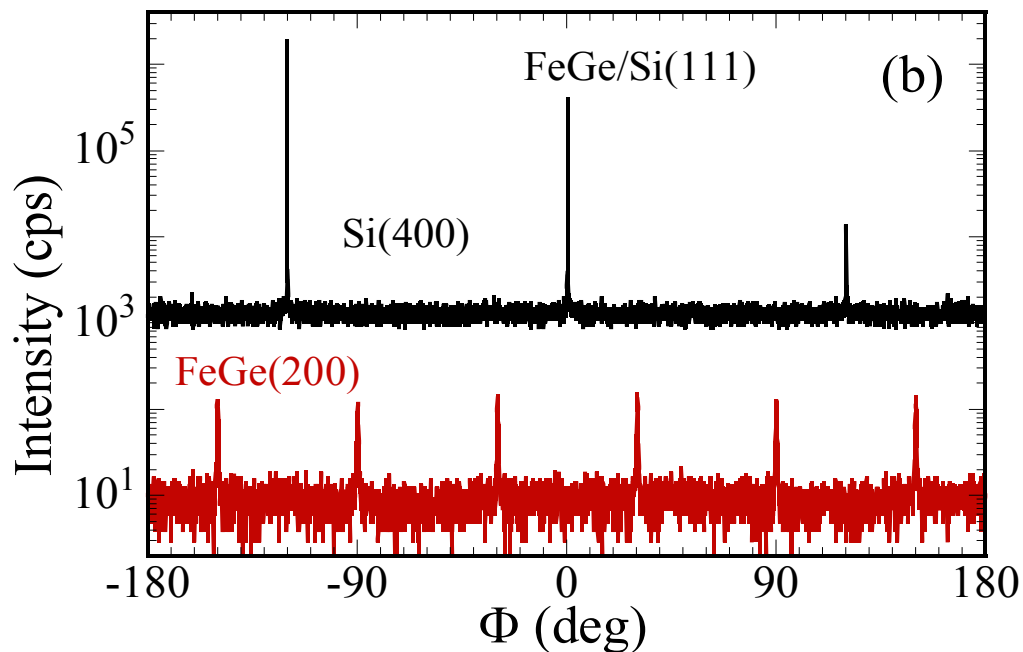


Pure B20 phase

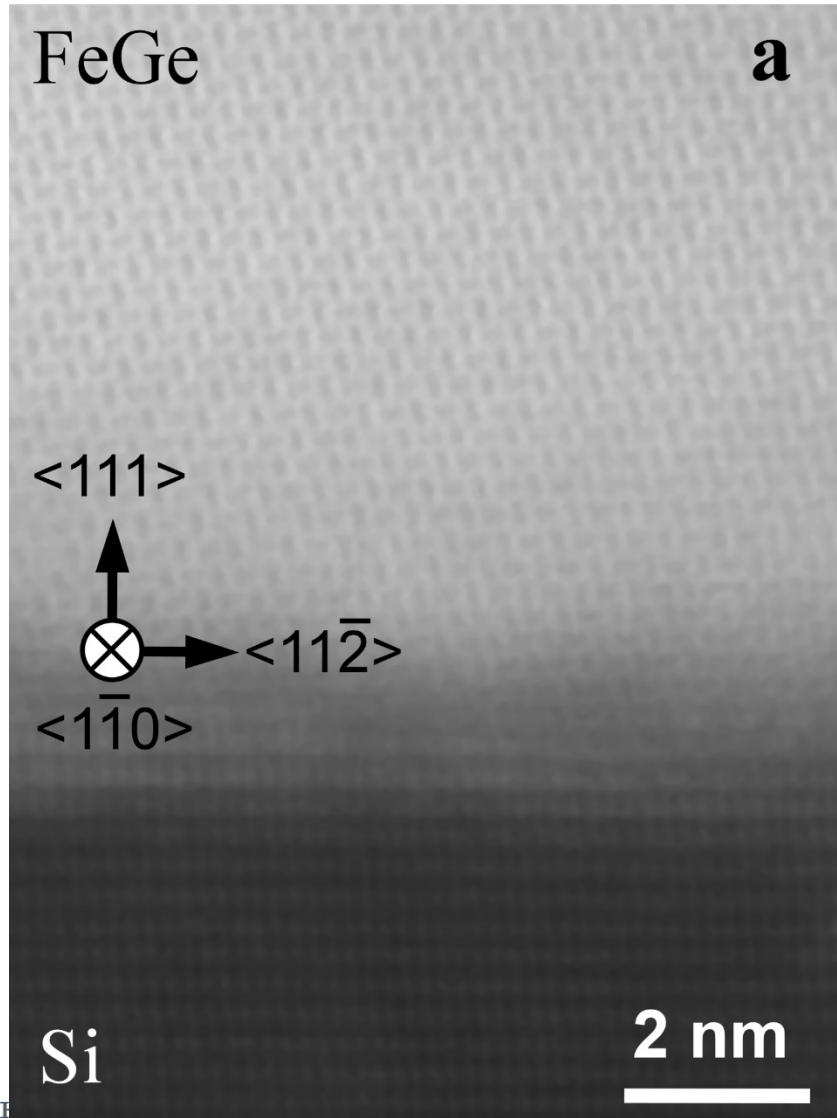
X-Ray Diffraction of FeGe films



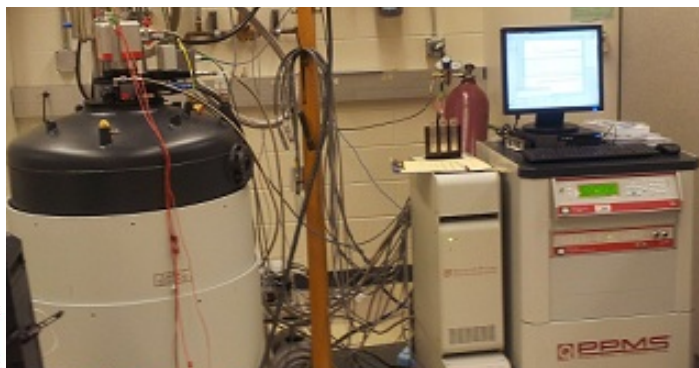
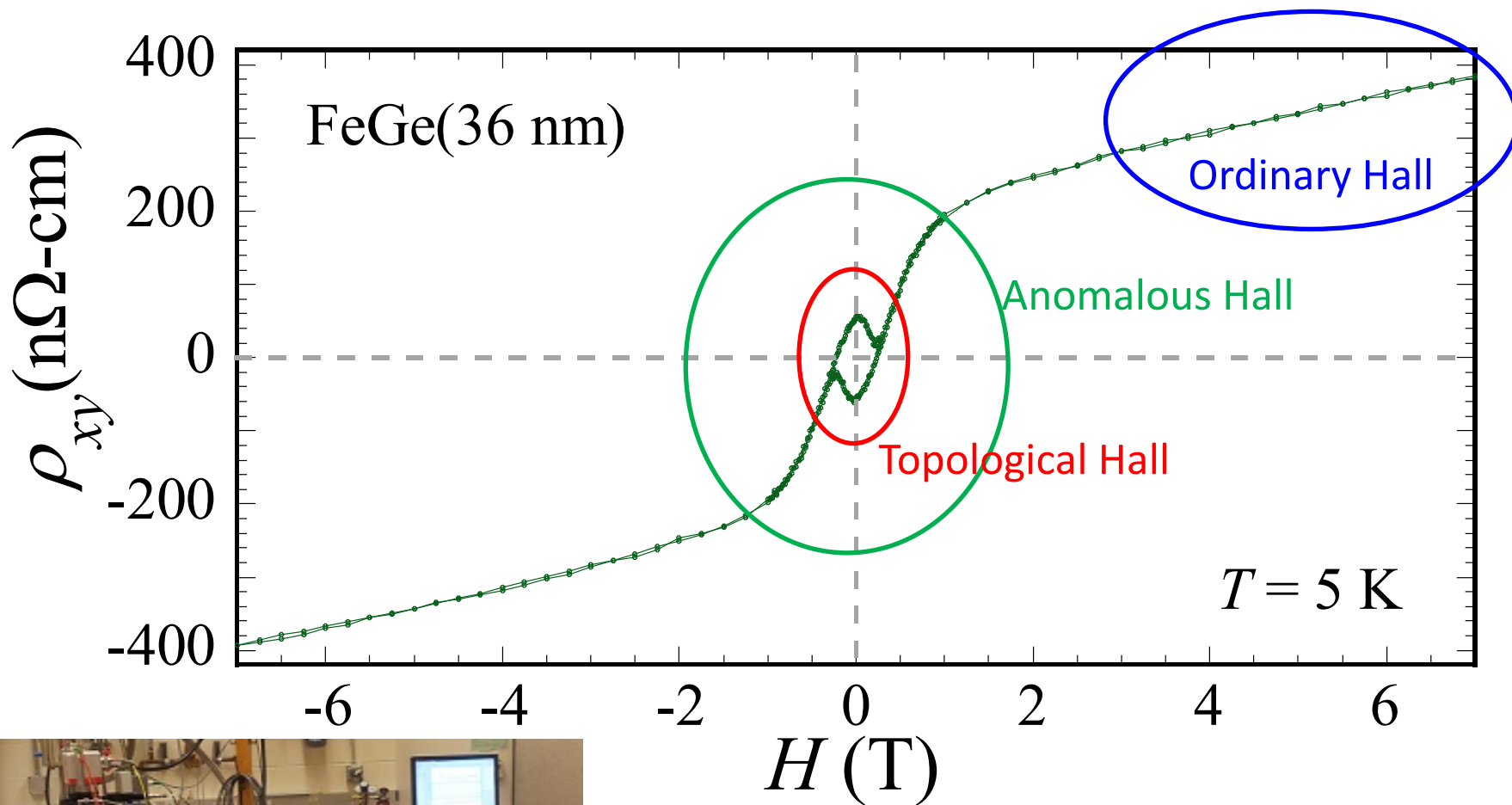
- Fully epitaxial
- 30° rotation



STEM imaging of FeGe films



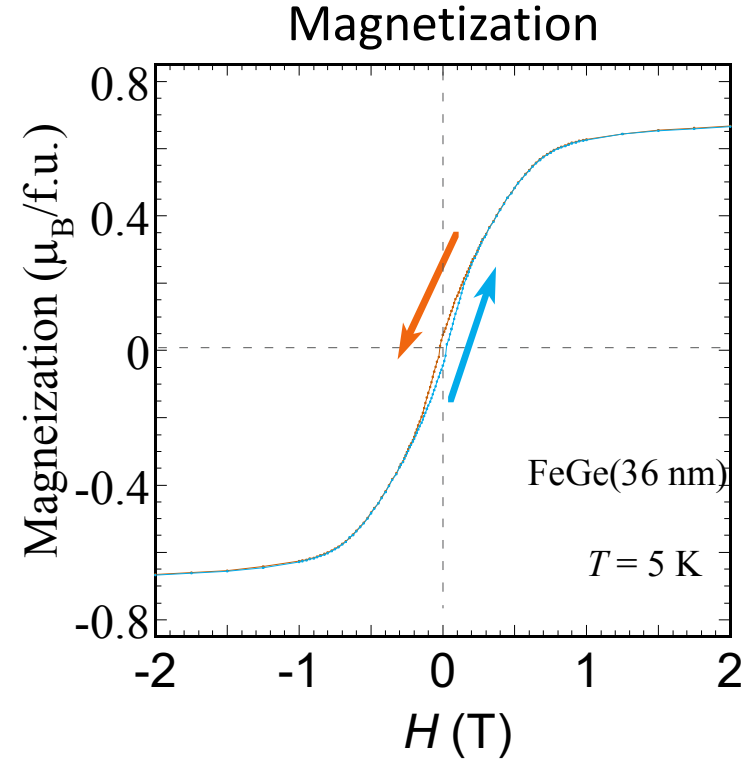
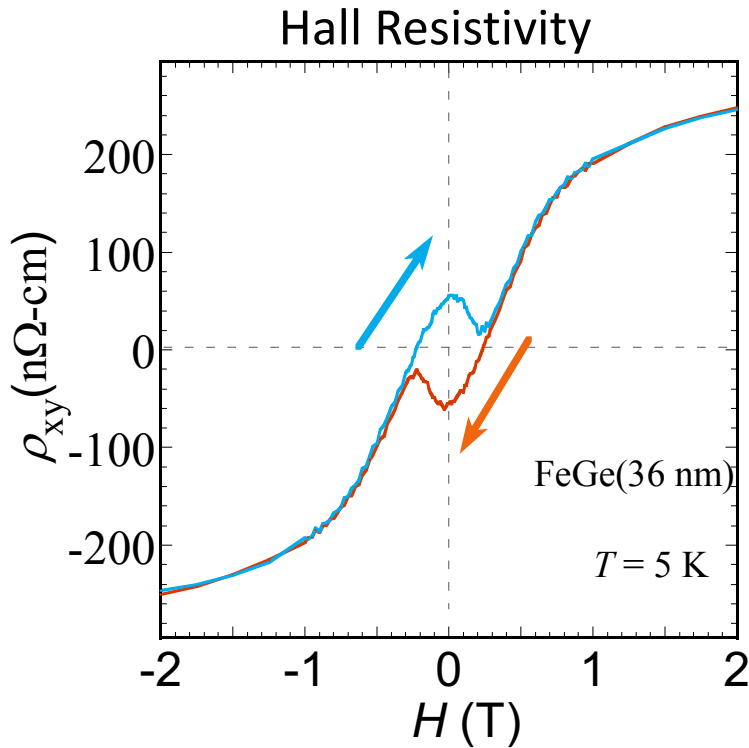
Hall resistivity in FeGe films



$$\rho_{xy} = R_0 H + R_s M + \rho_{TH}$$



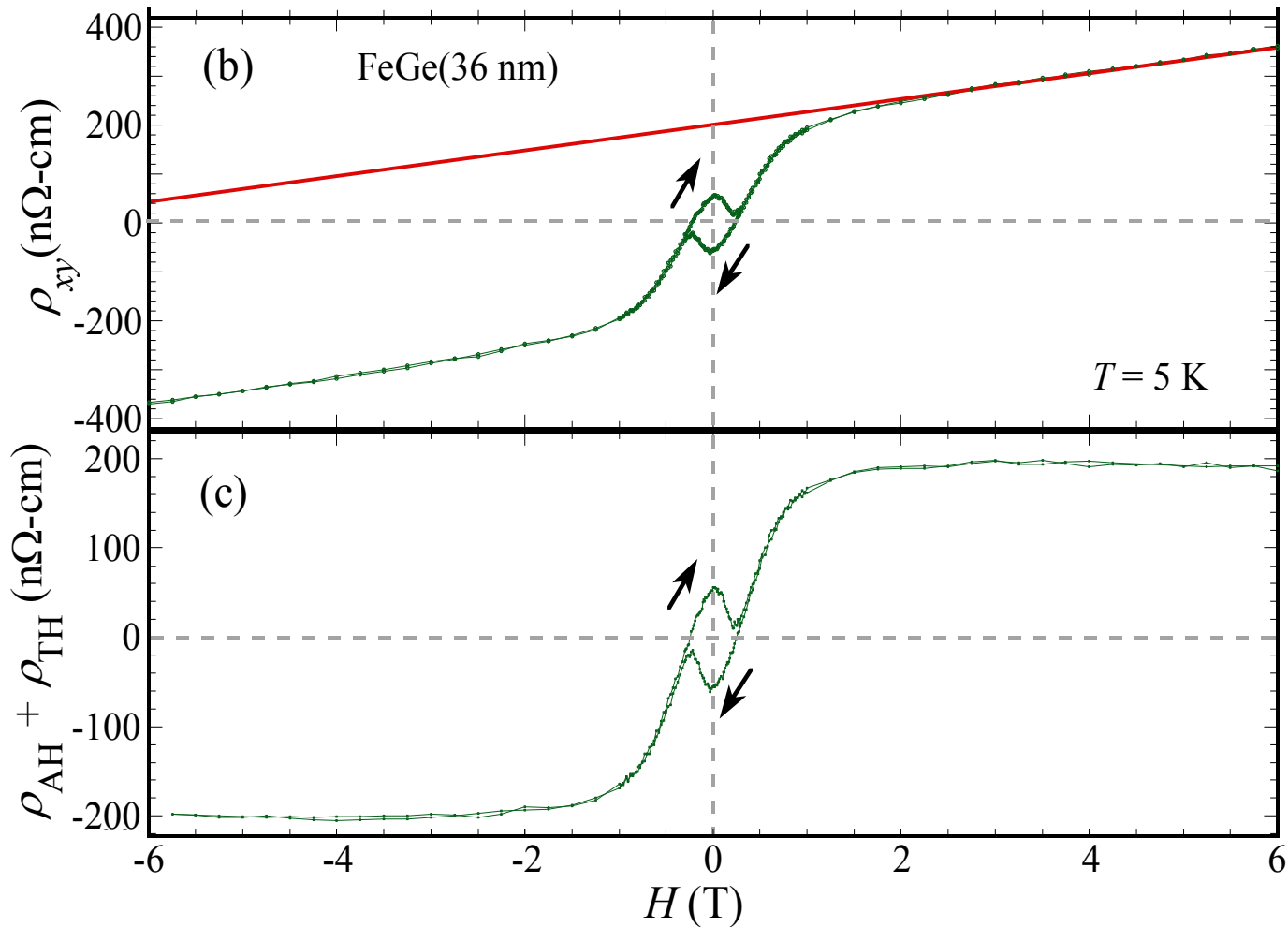
Hall resistivity in FeGe films



$$\rho_{xy} = R_0 H + R_s M + \rho_{TH}$$

Extracting topological Hall resistivity

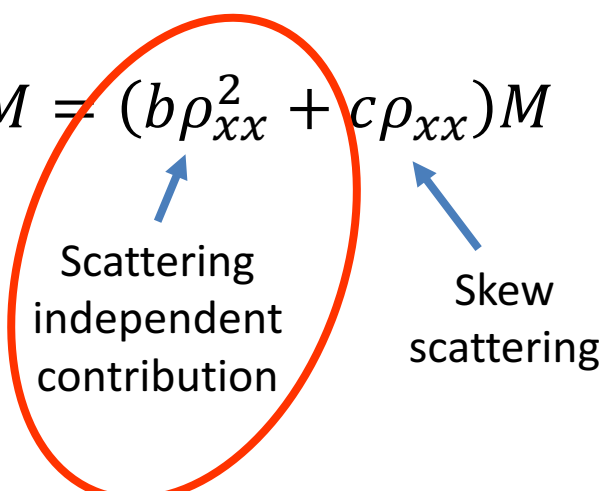
$$\rho_{xy} = R_0 H + R_S M + \rho_{TH}$$



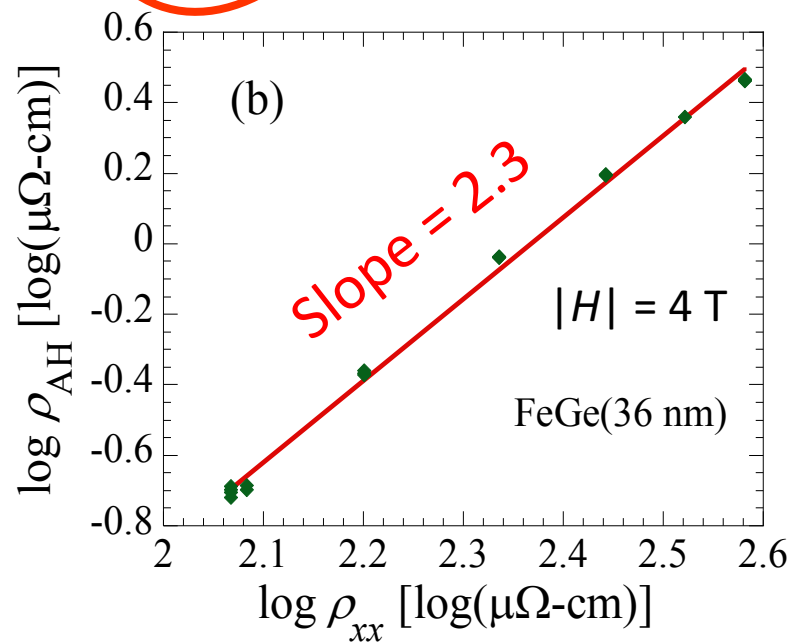
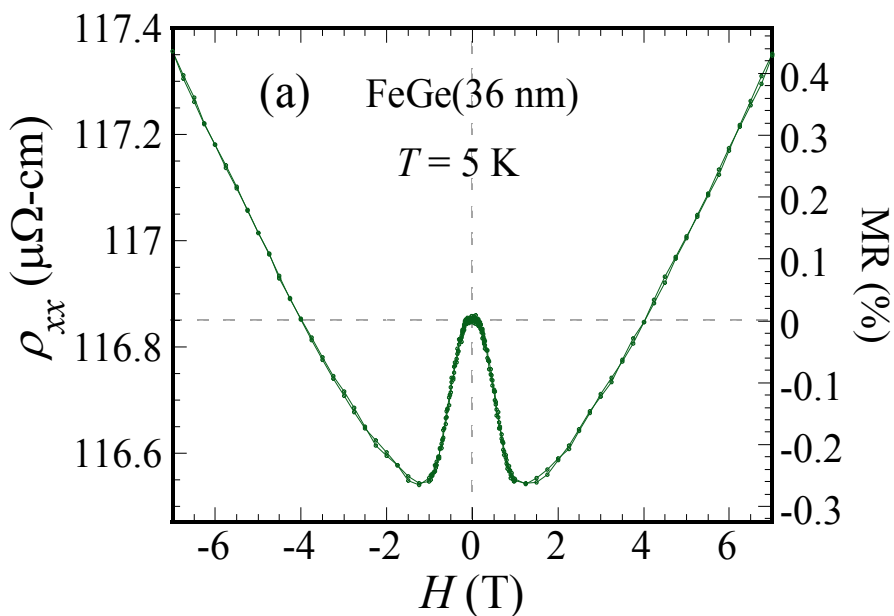
Extracting topological Hall resistivity

$$\rho_{xy} = R_0 H + R_S M + \rho_{TH}$$

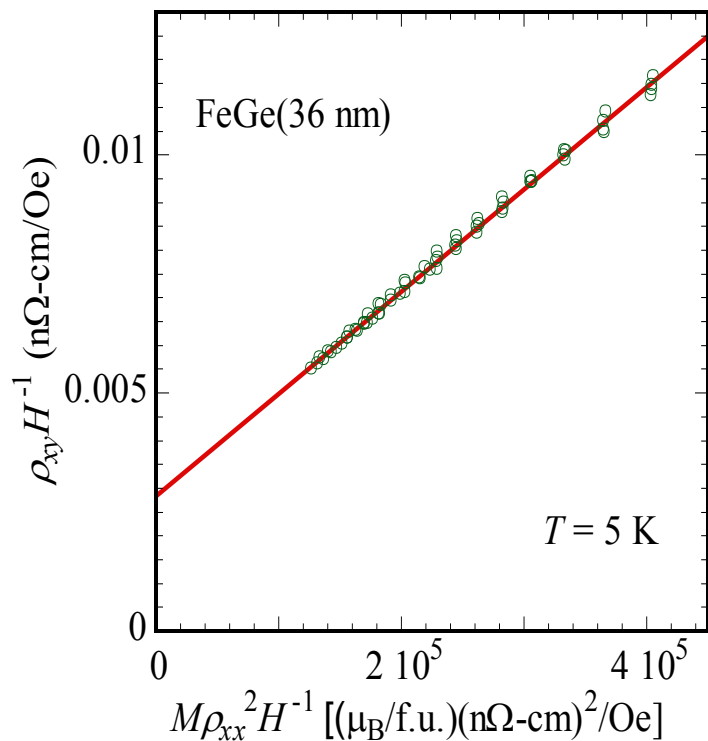
$$R_S M = (b\rho_{xx}^2 + c\rho_{xx})M$$



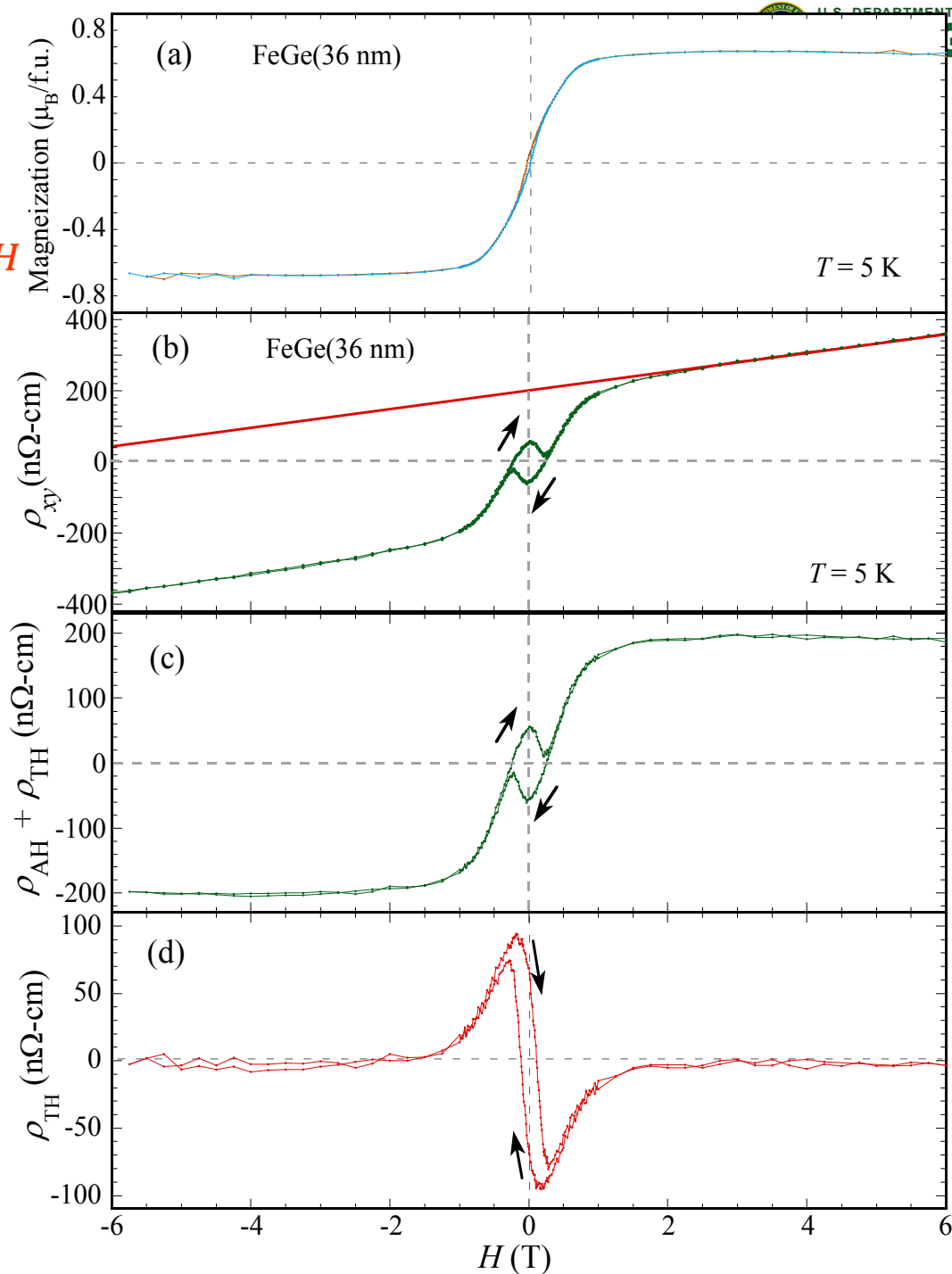
Small MR



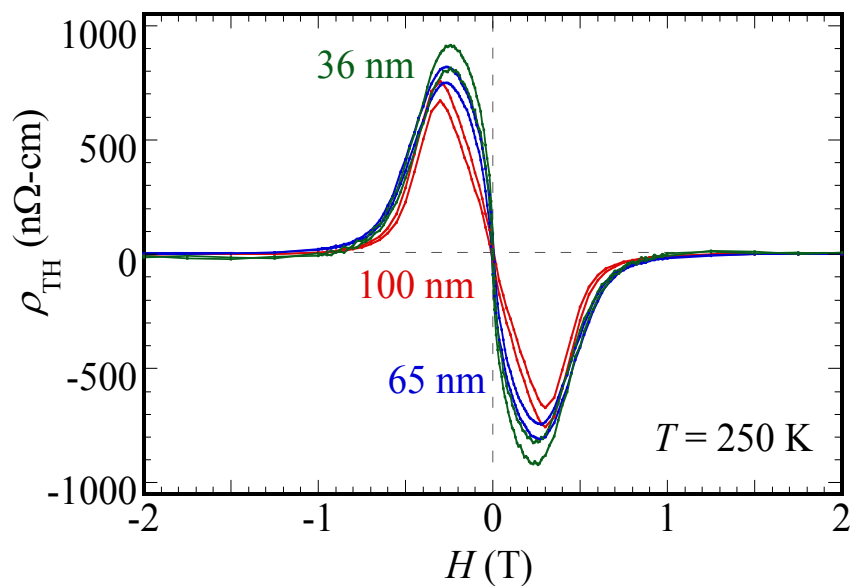
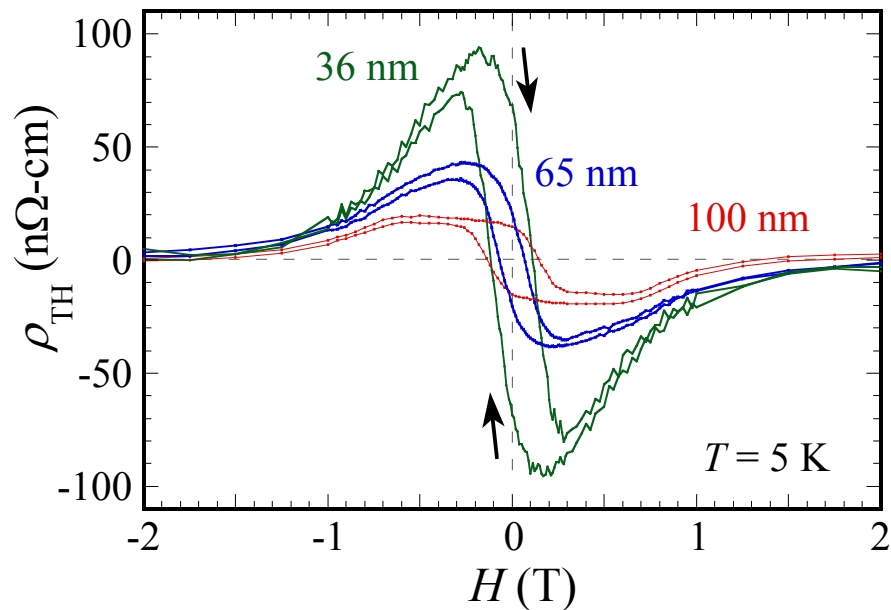
$$\rho_{xy} = R_0 H + b \rho_{xx}^2 M + \rho_{TH}$$



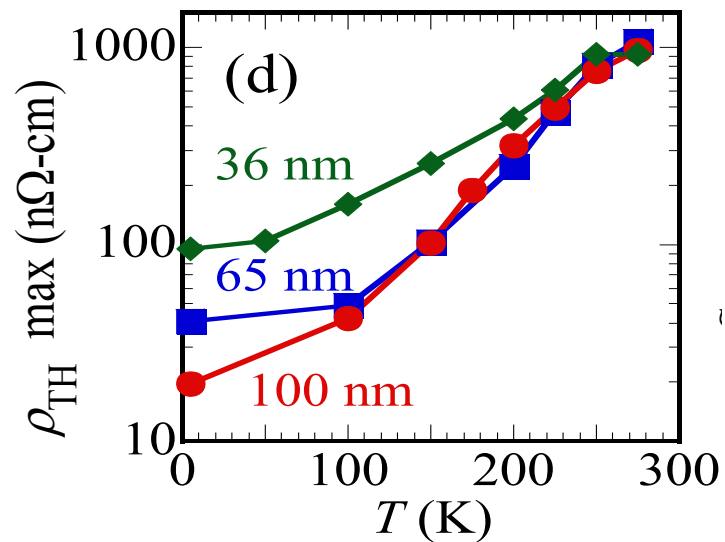
$$\frac{\rho_{xy}}{H} = R_0 + b \frac{\rho_{xx}^2 M_S}{H}$$



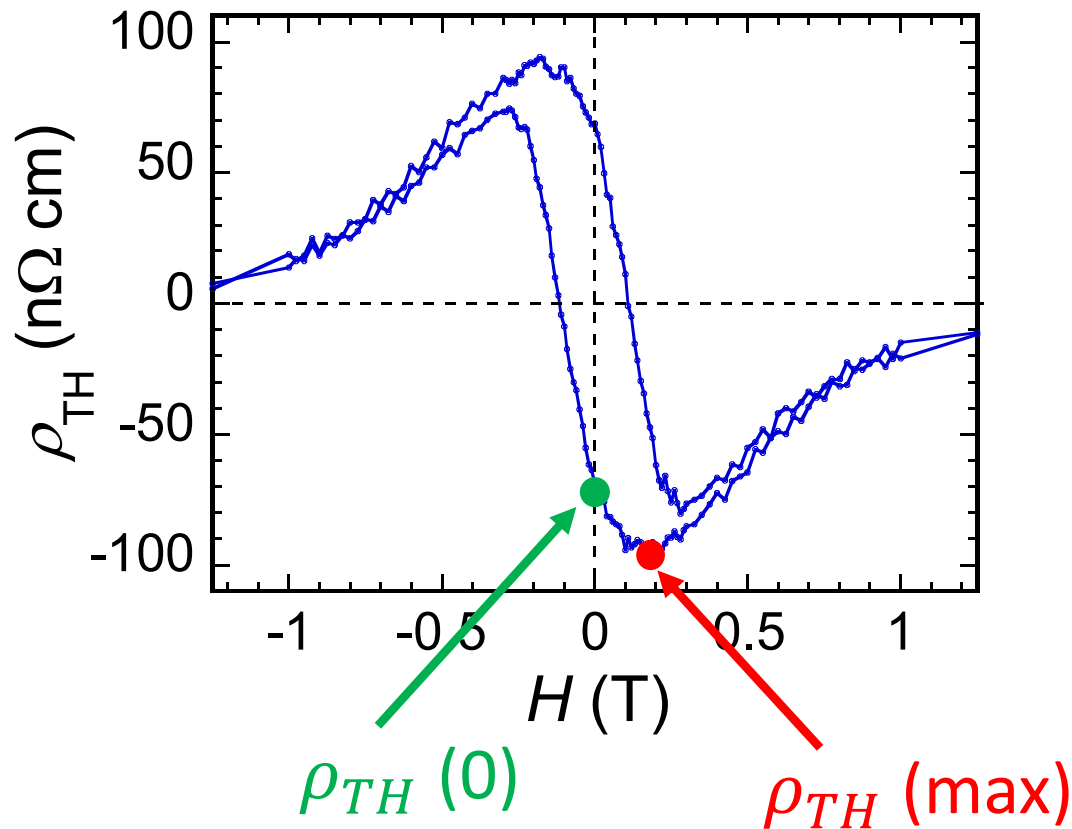
Extracted Topological Hall Resistivity



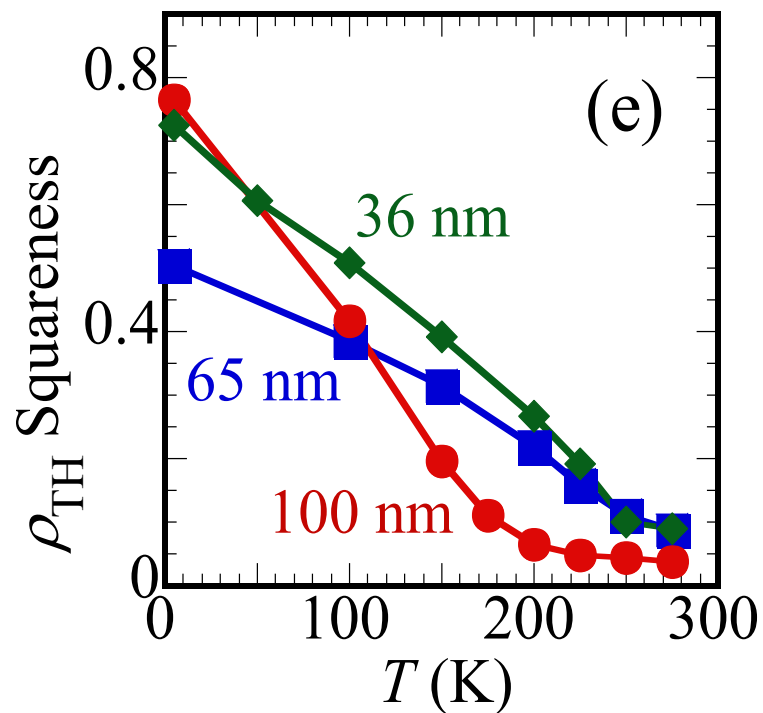
- Large topological Hall resistivity (up to 970 n Ω -cm)
- 6x larger than previous results



Remanent Topological Hall Resistivity

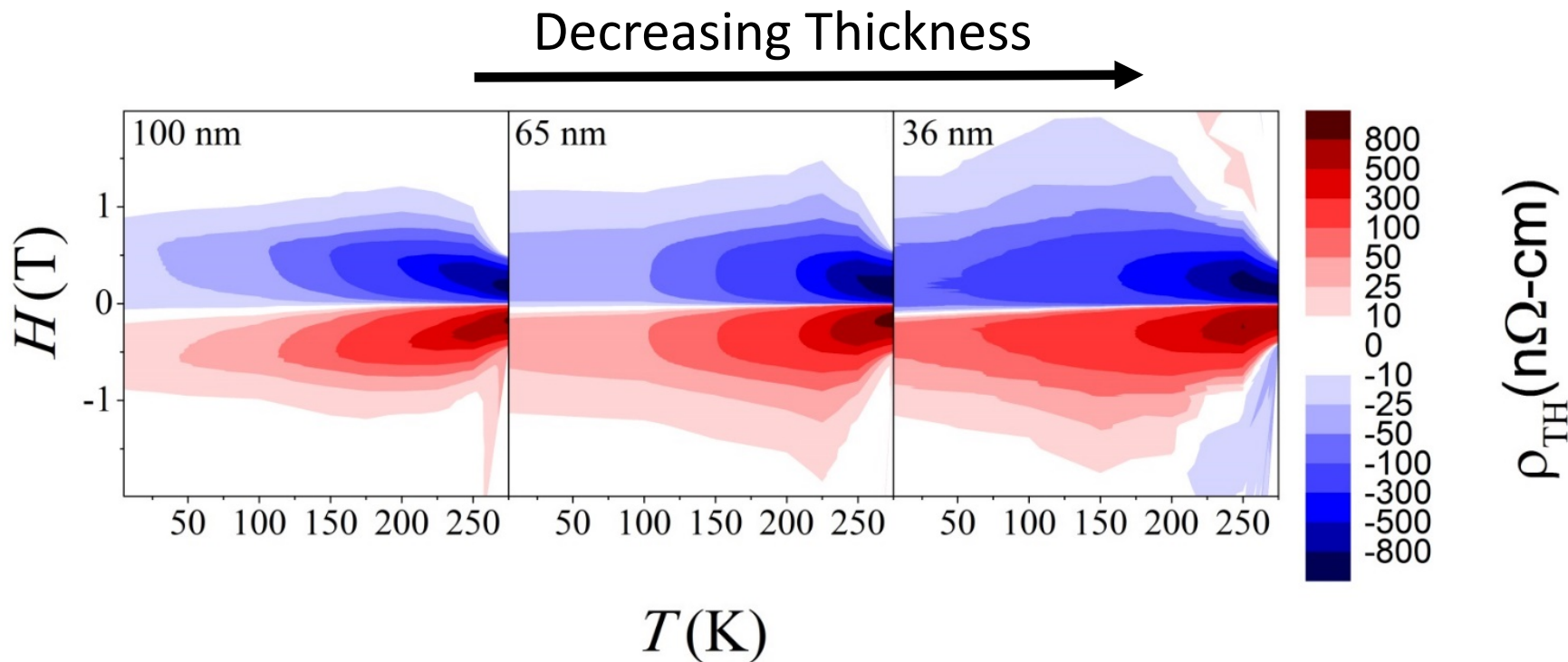


$\text{Squareness} \equiv \rho_{TH}(H = 0) / \rho_{TH}(\text{max})$



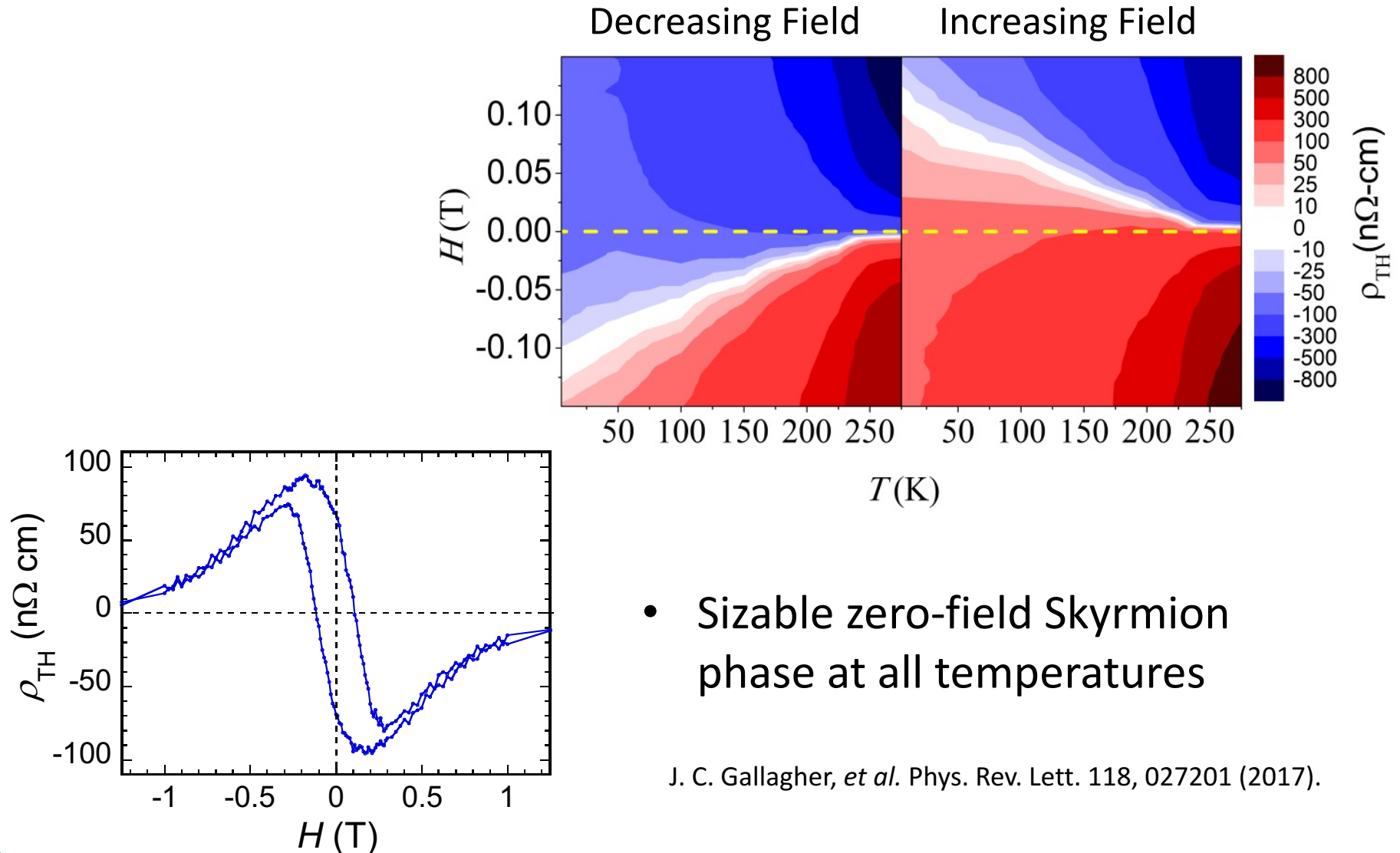
- Robust zero-field Skyrmion phase at all temperatures
- Squareness as high as 0.78

Topological Hall Effect: variable Temperatures



- Topological Hall effect detected up to $H = 2$ T
- Enhanced topological Hall effect at lower thicknesses
- Evidence for robust skyrmions at zero field

Zero-Field Topological Hall Effect



- Sizable zero-field Skyrmion phase at all temperatures

J. C. Gallagher, *et al.* Phys. Rev. Lett. 118, 027201 (2017).

Interface-driven skyrmions

ARTICLES

PUBLISHED ONLINE: 19 SEPTEMBER 2016 | DOI: 10.1038/NPHYS3883

nature
physics

Direct observation of the skyrmion Hall effect

Wanjun Jiang^{1,2,3*†}, Xichao Zhang^{4†}, Guoqiang Yu⁵, Wei Zhang^{1,6}, Xiao Wang⁷,
M. Benjamin Jungfleisch¹, John E. Pearson¹, Xuemei Cheng⁷, Olle Heinonen^{1,8}, Kang L. Wang⁵,
Yan Zhou⁴, Axel Hoffmann^{1*} and Suzanne G. E. te Velthuis^{1*}

Jiang, *et al. Nature Phys.* **13**, 162-169 (2016).

Ta(5 nm)
CoFeB(1.1 nm)
TaO_x (3 nm)

ARTICLES

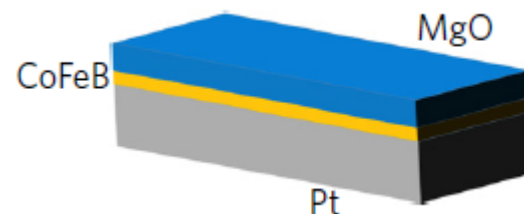
PUBLISHED ONLINE: 26 DECEMBER 2016 | DOI: 10.1038/NPHYS4000

nature
physics

Skyrmion Hall effect revealed by direct time-resolved X-ray microscopy

Kai Litzius^{1,2,3}, Ivan Lemesh⁴, Benjamin Krüger¹, Pedram Bassirian¹, Lucas Caretta⁴, Kornel Richter¹,
Felix Büttner⁴, Koji Sato⁵, Oleg A. Tretiakov^{6,7}, Johannes Förster³, Robert M. Reeve¹,
Markus Weigand³, Iuliia Bykova³, Hermann Stoll³, Gisela Schütz³, Geoffrey S. D. Beach^{4*}
and Mathias Kläui^{1,2*}

Litzius, *et al. Nature Phys.* **13**, 170-176 (2016).



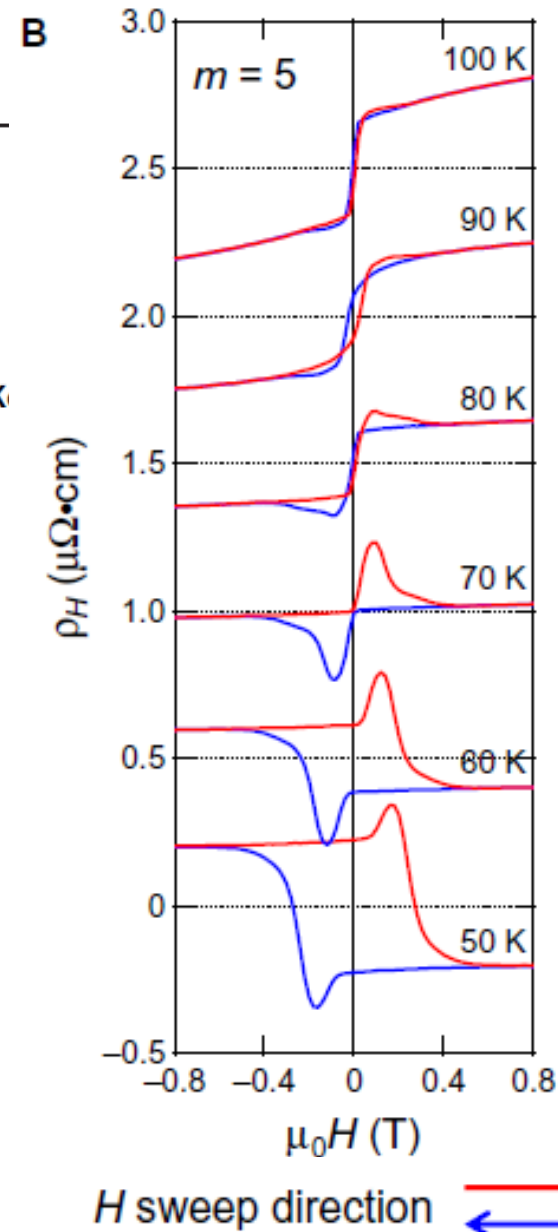
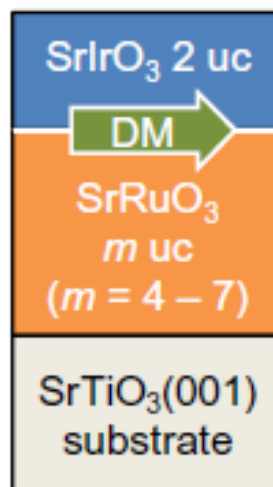
Skymions in oxide bilayers

RESEARCH ARTICLE

ELECTROMAGNETISM

Interface-driven topological Hall effect in SrRuO₃-SrIrO₃ bilayer

Jobu Matsuno,^{1*} Naoki Ogawa,¹ Kenji Yasuda,² Fumitaka Kagawa,¹ Wataru K. Yoshinori Tokura,^{1,2} Masashi Kawasaki^{1,2}



Matruno et al., *Science Advances* 2 : e1600304 (2016)

Skyrmions in oxide bilayers

RESEARCH ARTICLE

ELECTROMAGNETISM

Interface-driven topological Hall effect in SrRuO₃-SrIrO₃ bilayer

Jobu Matsuno,^{1*} Naoki Ogawa,¹ Kenji Yasuda,² Fumitaka Kagawa,¹ Wataru Koshihara,¹ Naoto Nagaosa,^{1,2} Yoshinori Tokura,^{1,2} Masashi Kawasaki^{1,2}

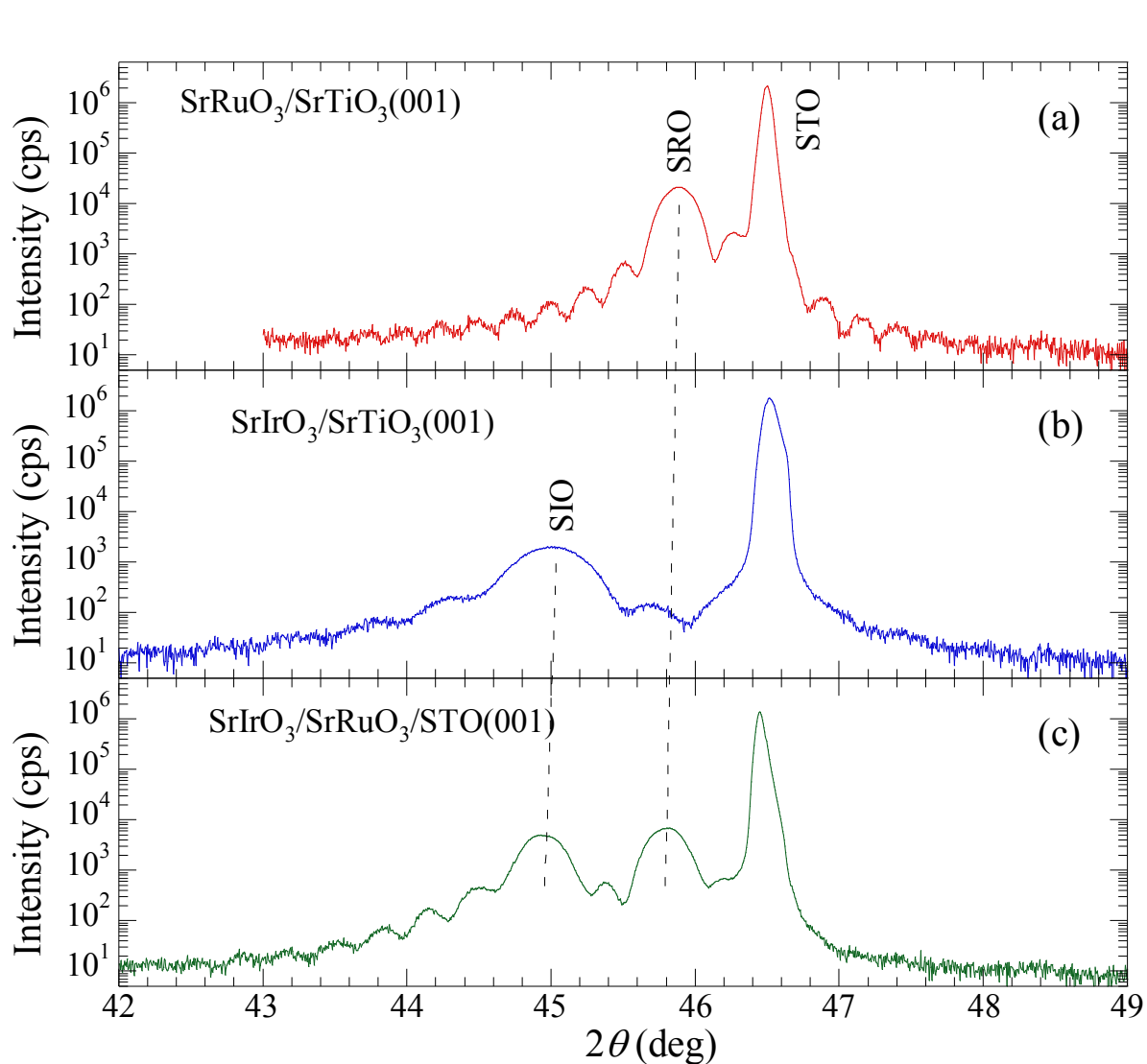
2016 © The Authors, some exclusive licensee American the Advancement of Science under a Creative Commons Attribution 4.0 International License. DOI: 10.1126/sciadv.1600304

“Such interaction is expected to realize a 10-nm-sized magnetic skyrmion.”

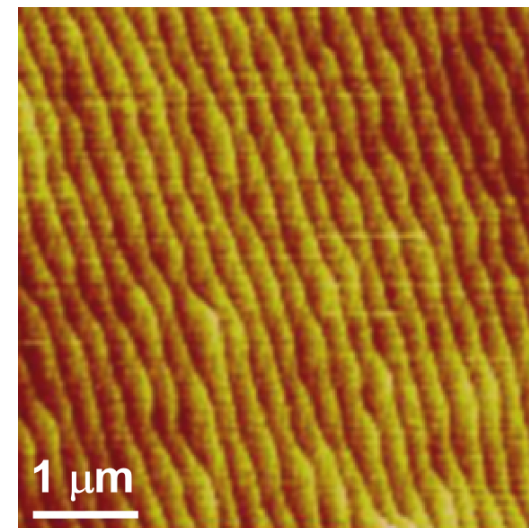
the $m \leq 6$ samples. The real $|D|$ value defined at the interface is thus deduced to be $m|D_{\text{eff}}| = 14$ meV. This is much larger than those in the interface between metals: -2.2 meV for permalloy/Pt (39) and -1.05 meV for a Co/Ni multilayer on Pt(111) (16).

Matruno et al., *Science Advances* 2 : e1600304 (2016)

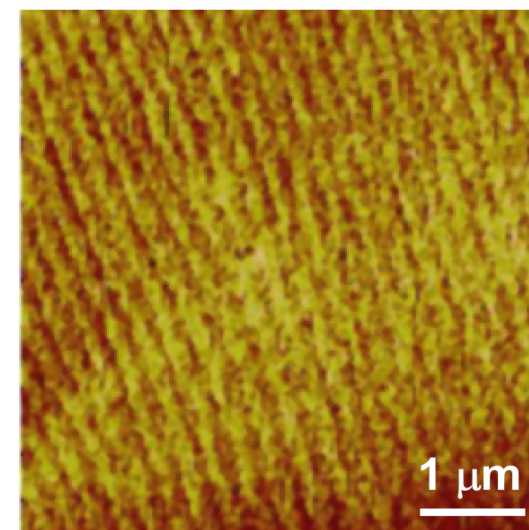
SrRuO₃/SrIrO₃ bilayers



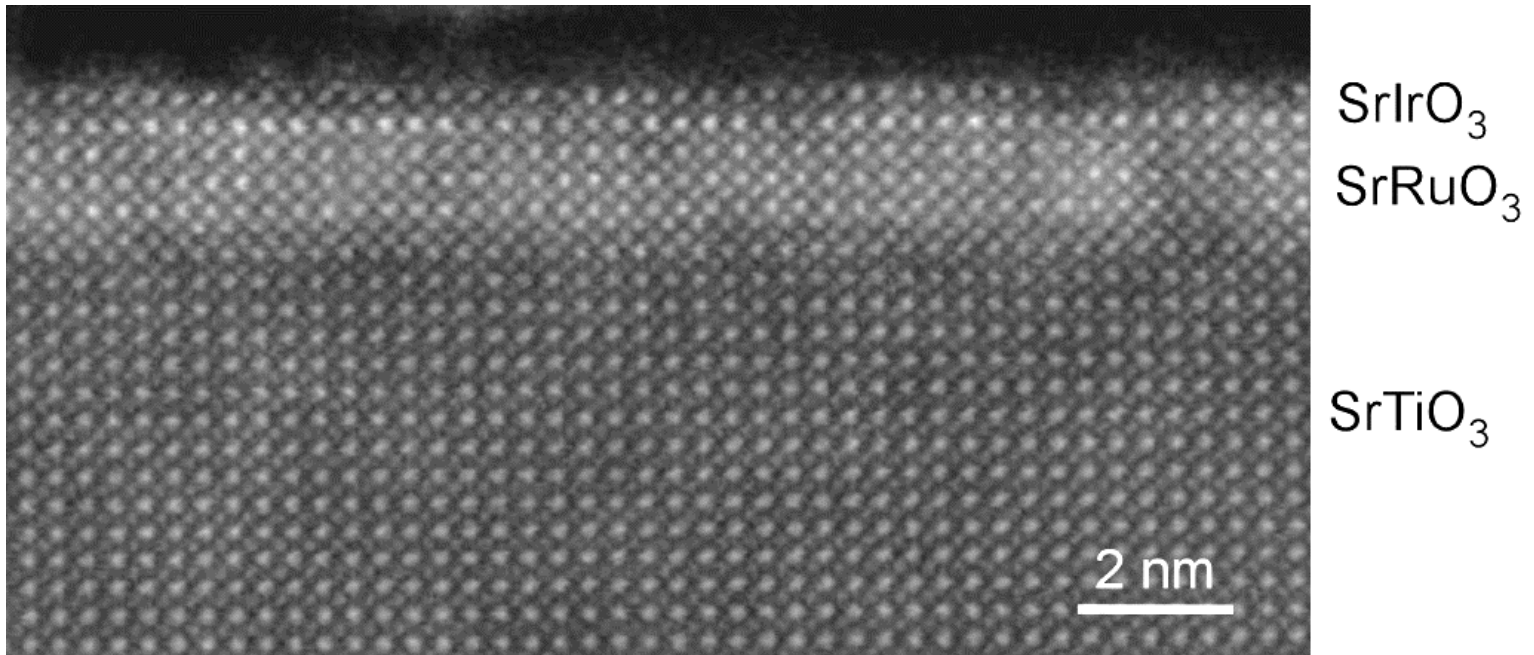
SrTiO₃ (001)



SrRuO₃(18 nm)/SrTiO₃ (001)



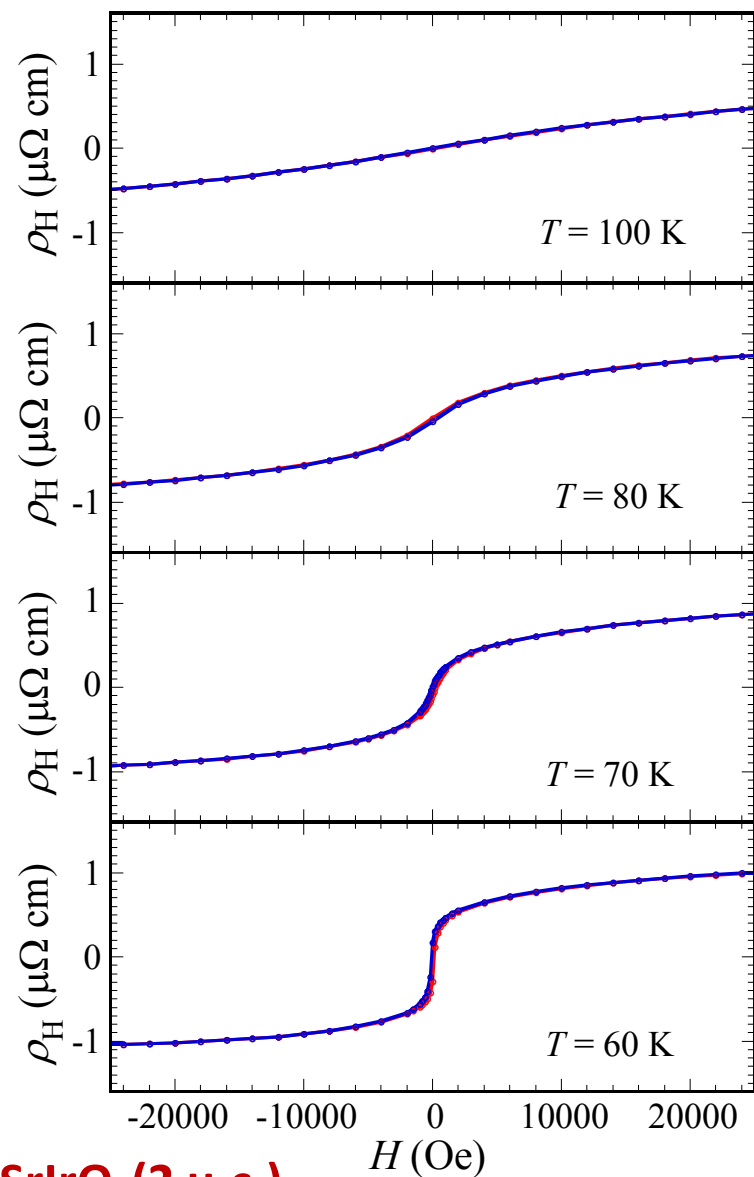
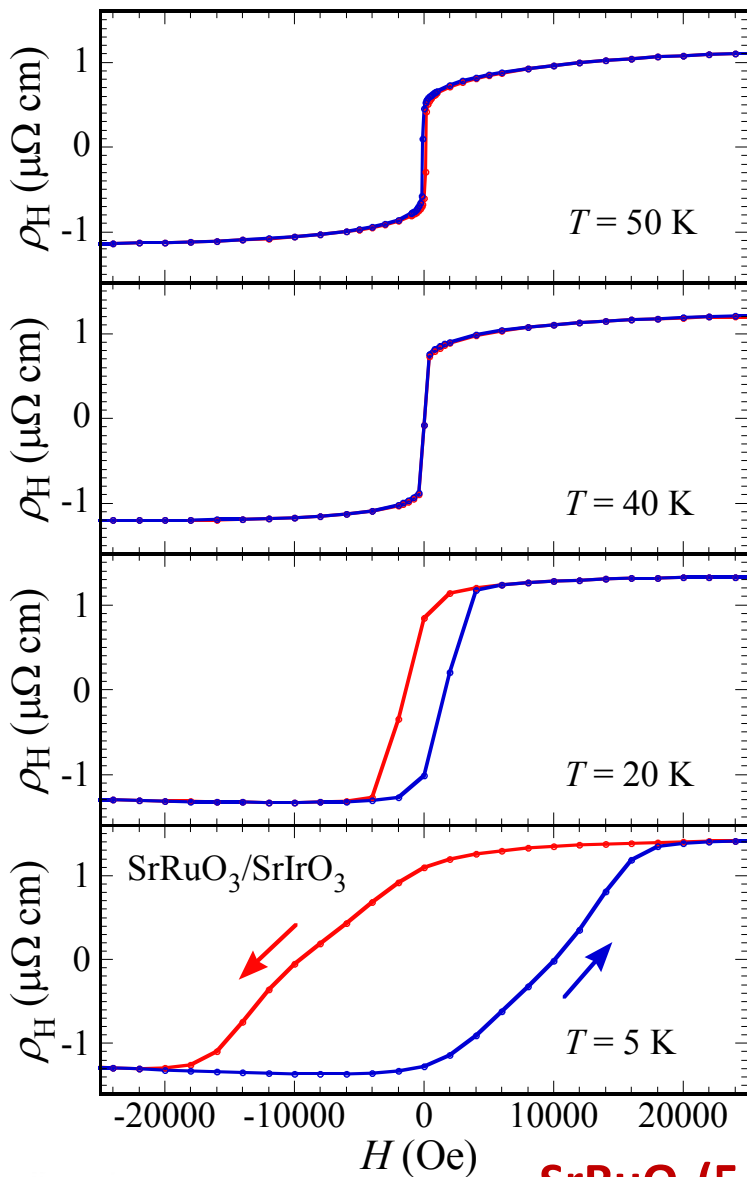
SrRuO₃/SrIrO₃ bilayers



SrRuO₃: FM with $T_C \sim 160$ K

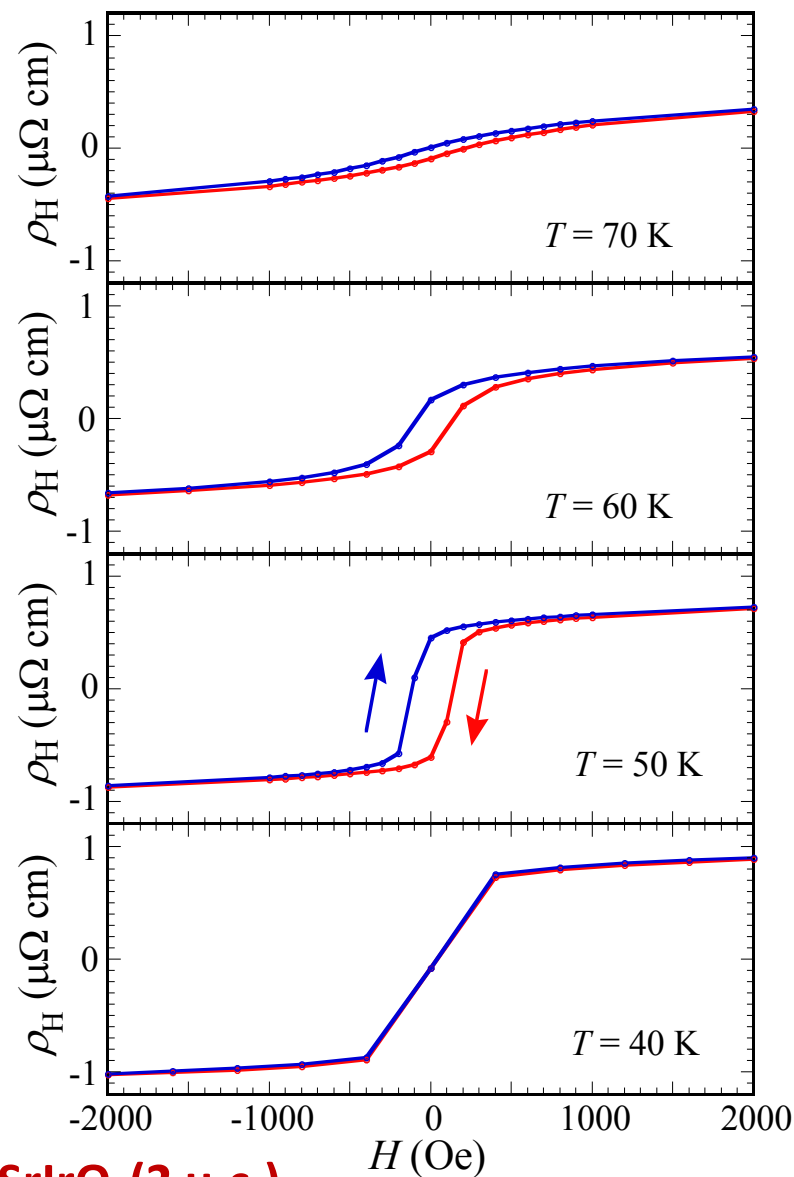
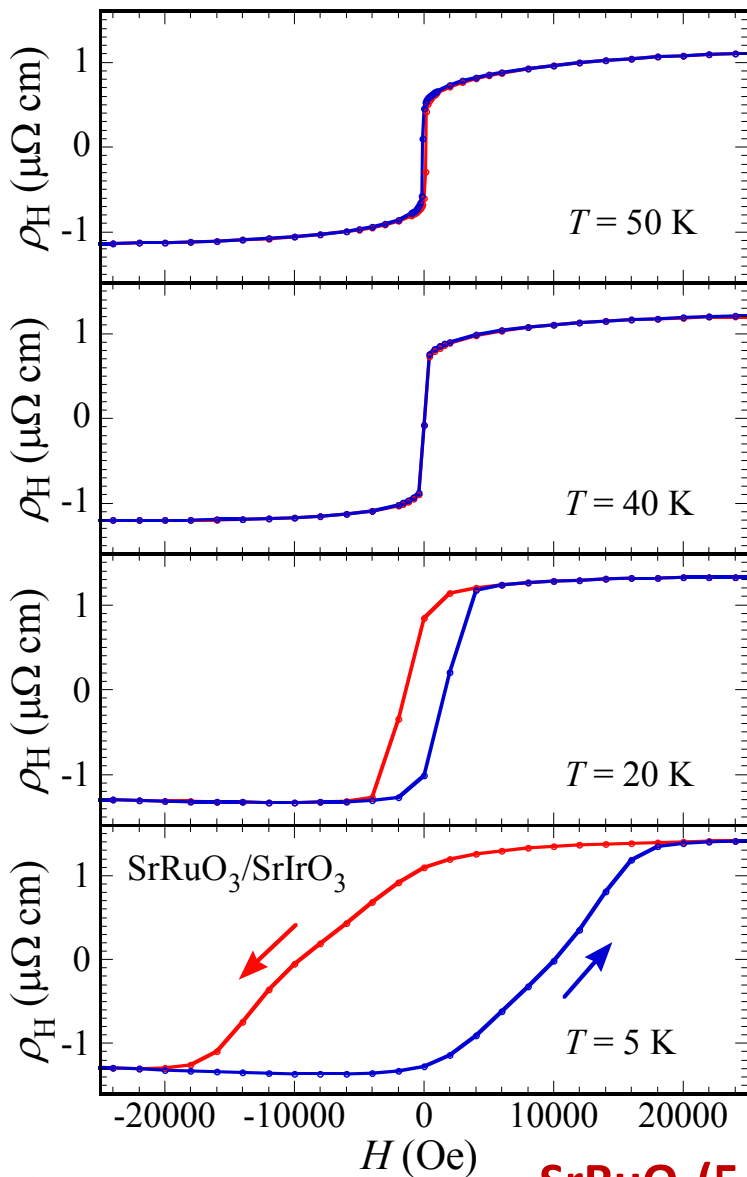
Esser & McComb (OSU)

Topological Hall Effect in SrRuO₃/SrIrO₃ bilayers



SrRuO₃(5 u.c.)/SrIrO₃(2 u.c.)

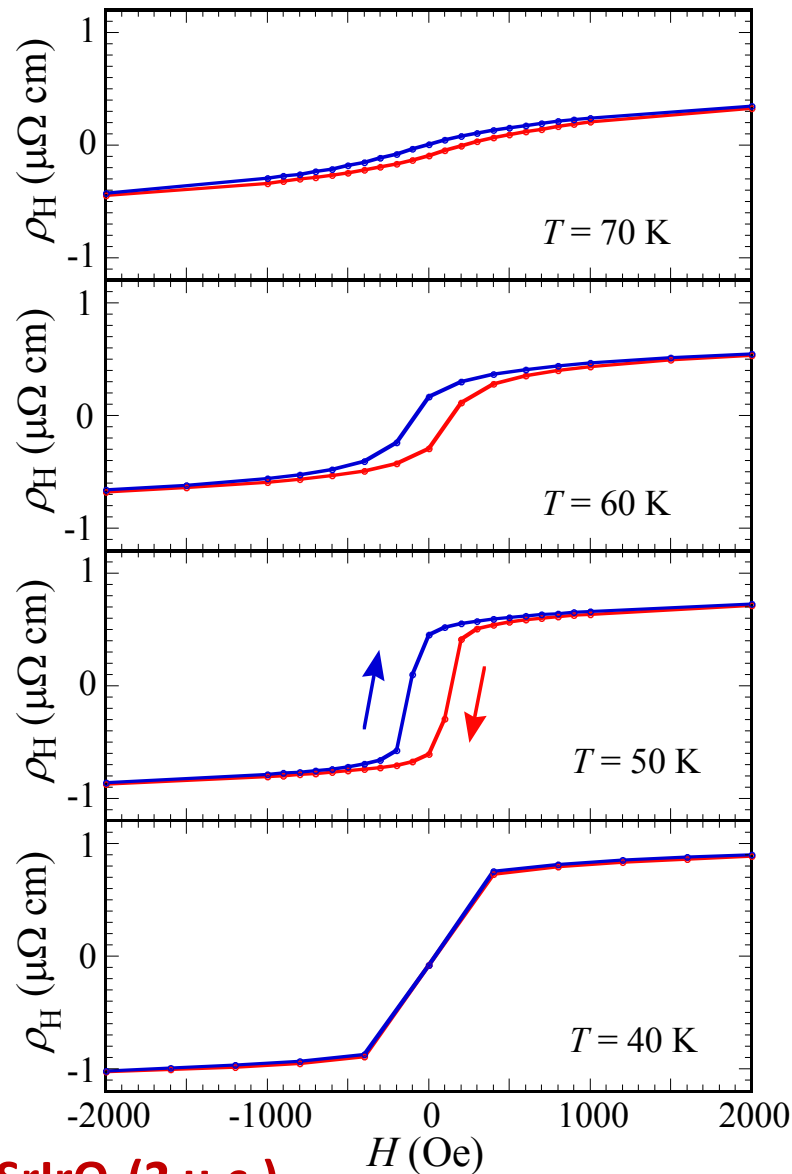
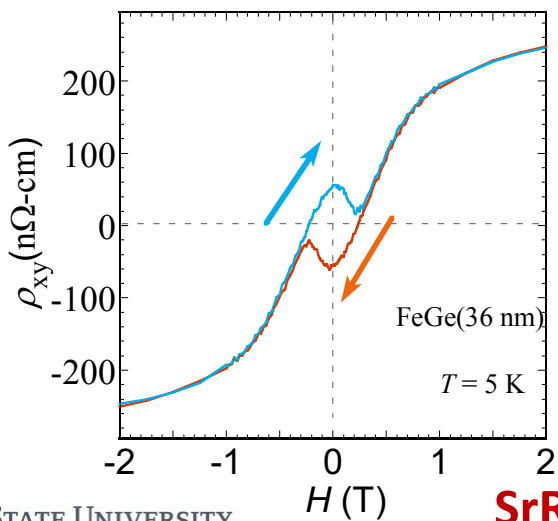
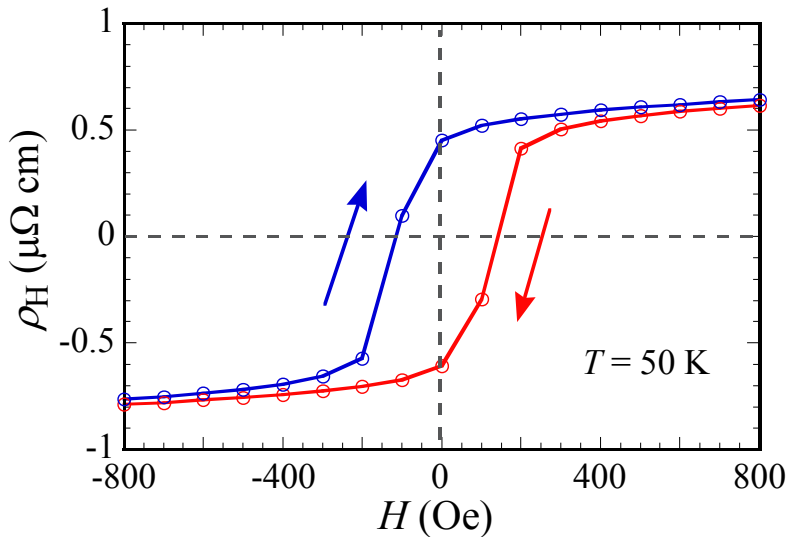
Topological Hall Effect in SrRuO₃/SrIrO₃ bilayers



SrRuO₃(5 u.c.)/SrIrO₃(2 u.c.)

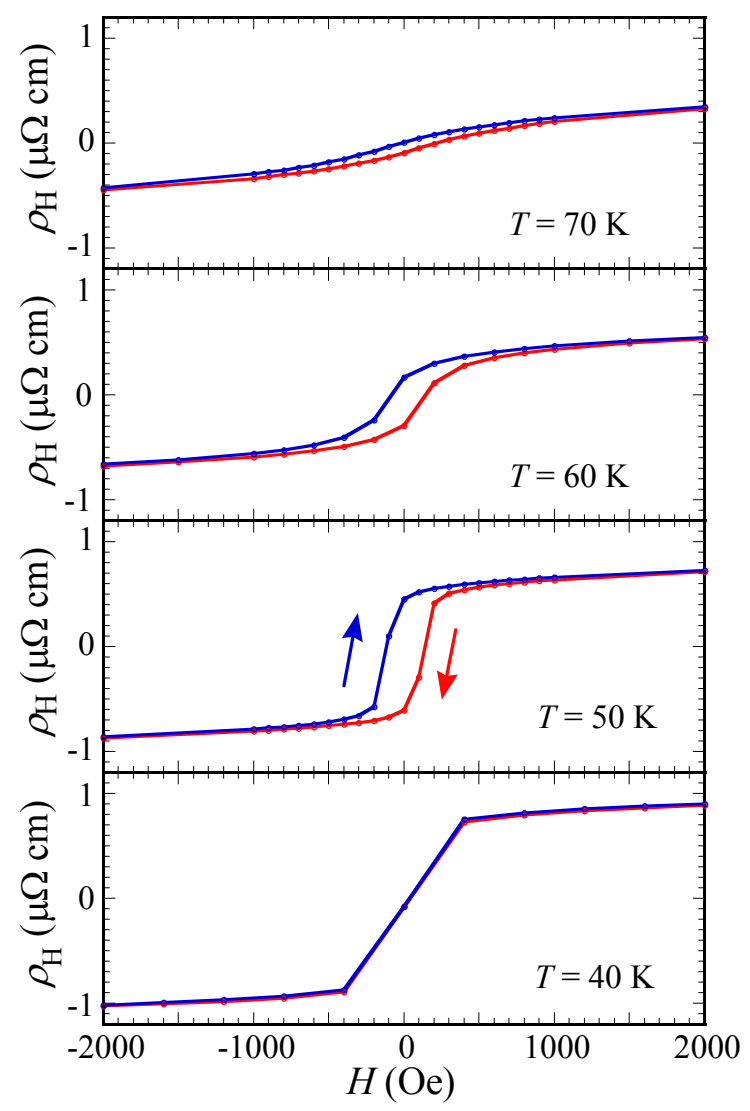
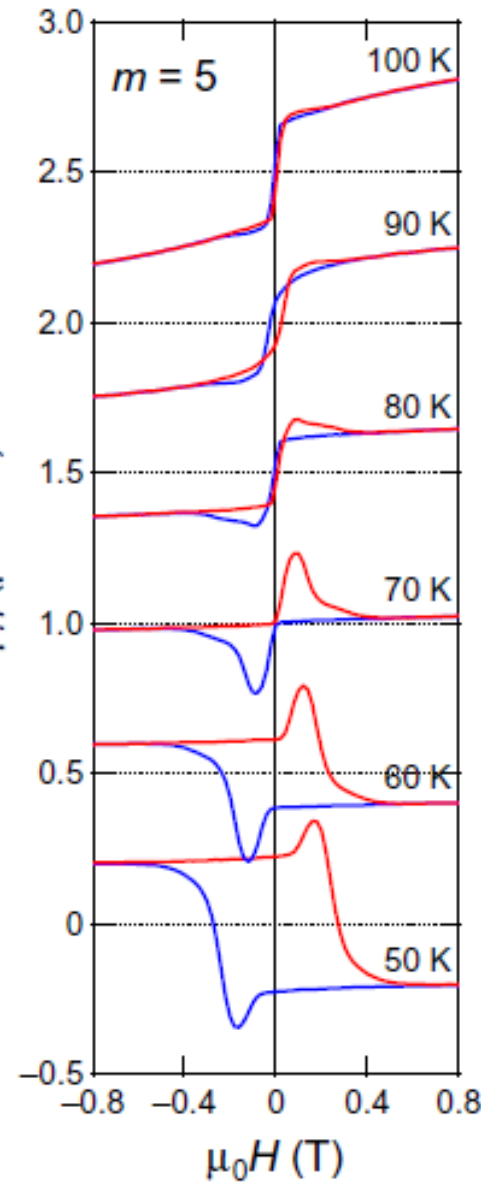
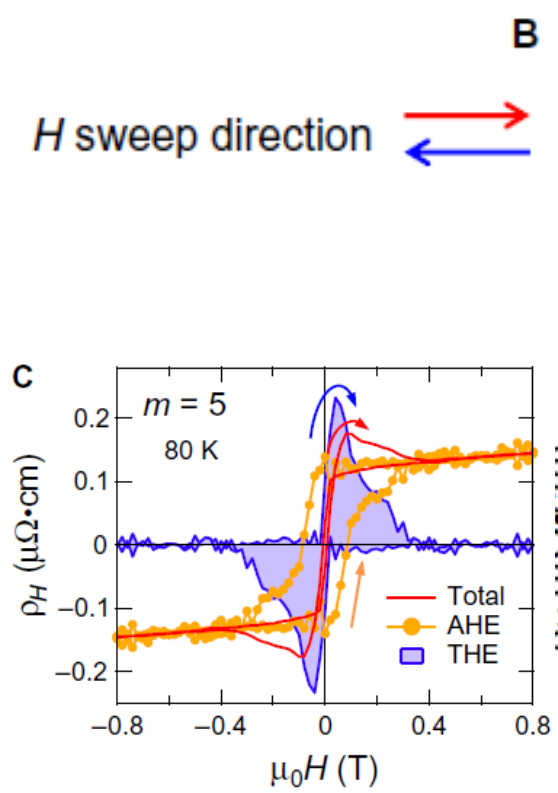
Topological Hall Effect in SrRuO₃/SrIrO₃ bilayers

Raw Hall resistivity



SrRuO₃(5 u.c.)/SrIrO₃(2 u.c.)

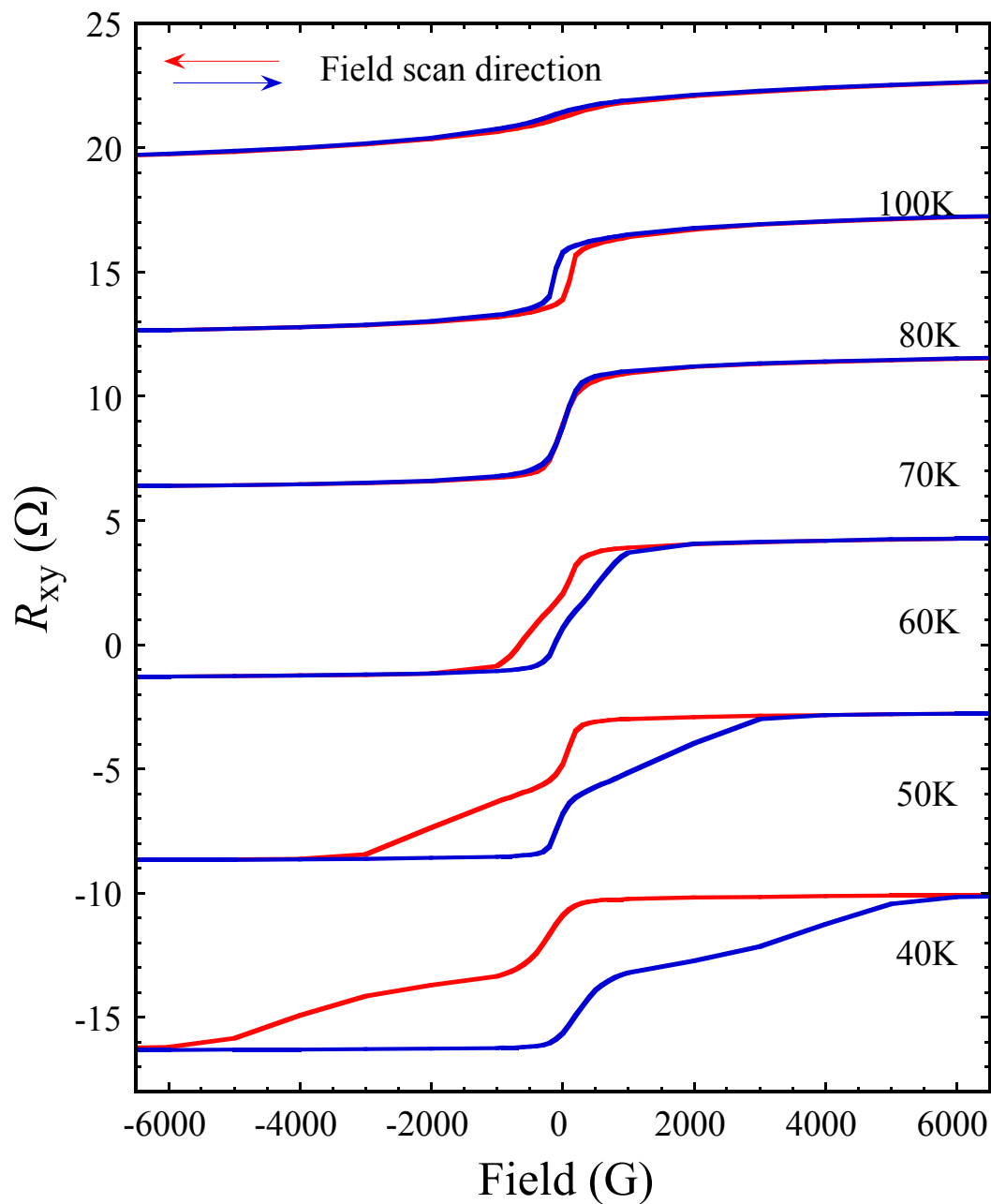
Topological Hall Effect in SrRuO₃/SrIrO₃ bilayers



Matruño et al.,
Science Advances
2:e1600304 (2015)

SrRuO₃(5 u.c.)/SrIrO₃(2 u.c.)

Single SrRuO₃ (6uc) layer on STO(001)



Room-temperature oxide skyrmions

- High- T_C FM oxides (LSMO, double perovskites)
- Strain-controlled anisotropy

“Such interaction is expected to realize a 10-nm-sized magnetic skyrmion.”

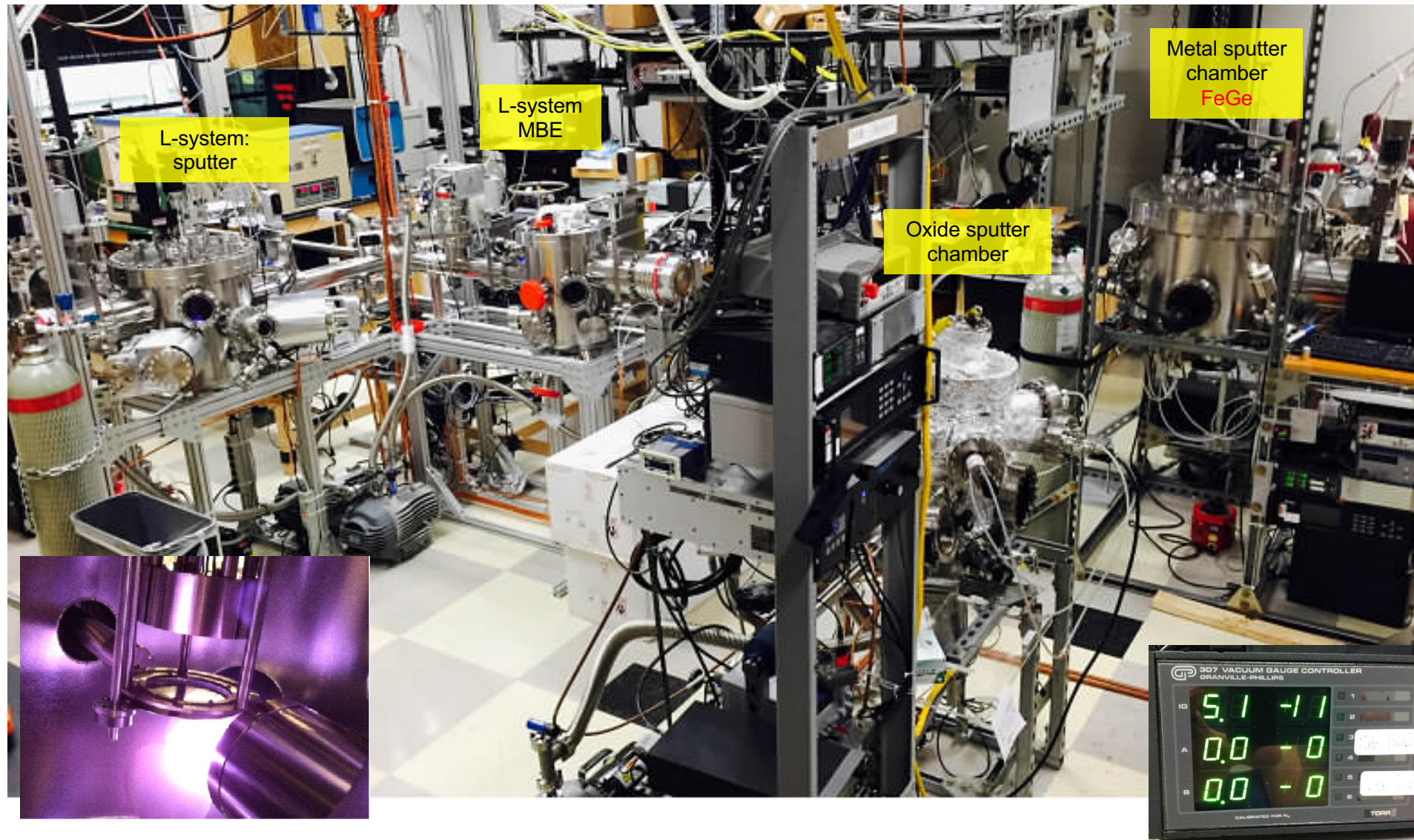
Matruno et al., *Science Advances* 2 : e1600304 (2016)

Summary

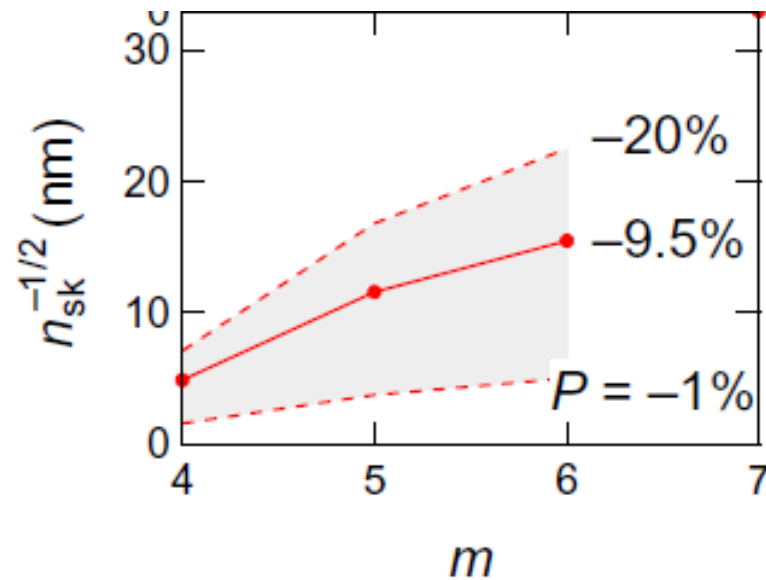
- Growth of pure B20 phase, epitaxial FeGe films using UHV off-axis sputtering
- Confirmation of the pure B20 crystal structure using XRD and STEM
- Large topological Hall resistivity up to 970 n Ω -cm
- Robust Skyrmion formation at zero field
- Skyrmions in oxide FM/NM bilayers



Sputter deposition of FeGe films



Skyrmions in oxide bilayers



$$\rho_H^T = PR_0 b = PR_0 n_{sk} \phi_0$$

The skyrmion number

The swirling structure of a skyrmion is characterized by the topological **skyrmion number defined by**

$$N_{\mathbf{k}} = \frac{1}{4\pi} \iint d^2\mathbf{r} \mathbf{n} \cdot \left(\frac{\partial \mathbf{n}}{\partial x} \times \frac{\partial \mathbf{n}}{\partial y} \right) \quad (B1)$$

as the integral of the solid angle, and counts how many times $\mathbf{n}(\mathbf{r}) = \mathbf{n}(x,y)$ wraps the unit sphere^{44,45}. Using the symmetry of the skyrmion, one can write

$$\mathbf{n}(\mathbf{r}) = (\cos\phi(\varphi)\sin\theta(r), \sin\phi(\varphi)\sin\theta(r), \cos\theta(r)) \quad (B2)$$

where we introduce the polar coordinates $\mathbf{r} = (r\cos\varphi, r\sin\varphi)$. Putting this form into equation (B1), we obtain

$$N_{\mathbf{k}} = \frac{1}{4\pi} \int_0^{2\pi} d\varphi \int_0^{\infty} dr \frac{d\theta(r)}{dr} \frac{d\phi(\varphi)}{d\varphi} \sin\theta(r) = [\cos\theta(r)]_{r=0}^{\infty} \int_0^{2\pi} d\varphi \frac{d\phi(\varphi)}{d\varphi}$$

Accordingly, one can classify the skyrmion structures as follows. Suppose the spins point up at $r \rightarrow \infty$ while they point down at $r = 0$. Then, $[\cos\theta(r)]_{r=0}^{\infty} = 2$. Now, there are several possibilities for $\phi(\varphi)$. The vorticity is defined by the integer $m = [\phi(\varphi)]_{\varphi=0}^{\varphi=2\pi} / 2\pi$. Therefore, the vorticity determines the skyrmion number as $N_{\mathbf{k}} = m$, once the boundary condition at $r \rightarrow \infty$ is fixed. We further define the helicity by the phase γ appearing in

$$\Phi(\varphi) = m\varphi + \gamma \quad (B3)$$

We show in Fig. 1g various skyrmion structures corresponding to vorticity $m = \pm 1$, and $\gamma = 0, \pm\pi/2$ and π . Fig. 1a corresponds to $m = 1$ and $\gamma = \pi/2$.

From equations (B2) and (B3), the magnetic charge $\rho_{\text{mag}} = \nabla \cdot \mathbf{n}$ is calculated as

$$\rho_{\text{mag}} = \cos[(m-1)\varphi + \gamma] \left(\frac{d\theta}{dr} \cos\theta + \frac{m}{r} \sin\theta \right)$$

On the other hand, the DM interaction is given by

$$H_{\text{DM}} = D\mathbf{n} \cdot (\nabla \times \mathbf{n}) = D\sin[(m-1)\varphi + \gamma] \left(\frac{d\theta}{dr} + \frac{m}{2r} \sin 2\theta \right)$$

or

$$H_{\text{DM}} = D\mathbf{n} \cdot (\mathbf{e}_z \times \nabla) \mathbf{n} = D\sin[(m-1)\varphi + \gamma] \left(\frac{d\theta}{dr} + \frac{m}{2r} \sin 2\theta \right)$$

Therefore, the state with vorticity $m = +1$ and $\gamma = \pm\pi/2$ has the lowest energy, where the sign of γ is determined by the sign of D , which in turn is determined by the crystal structure. (When the DM vector is rotated by $\pm\pi/2$, $\gamma = 0$ or π becomes the stable configuration¹⁰⁹.)

In the case of the four-spin interaction (case 3) or the frustrated exchange interaction (case 4), there is no distinction between the skyrmion and anti-skyrmion, that is, $m = \pm 1$ and γ can take an arbitrary value.

Emergent electromagnetic field

One can describe the interaction between the spin textures and the conduction electrons in terms of the EEMF expressed by the spin directions. We consider the double-exchange

model where the conduction electrons and spins are coupled **ferromagnetically at each site** by Hund's rule coupling. In the strong coupling limit, the spin wavefunction $|\chi(\mathbf{r})\rangle$ of the conduction electron at \mathbf{r} corresponding to the localized spin $\mathbf{n}(\mathbf{r})$ in equation (B2) is given by

$$|\chi(\mathbf{r})\rangle = \left(\cos \frac{\Theta(\mathbf{r})}{2}, e^{i\phi(\mathbf{r})} \sin \frac{\Theta(\mathbf{r})}{2} \right)^T$$

where T means the transpose. Therefore, when a conduction electron hops between two sites \mathbf{r} and $\mathbf{r} + c\mathbf{n}_k$ (\mathbf{n}_k is the unit vector along $\alpha(=x,y,z)$ direction, α is the space index and c a lattice constant), the matrix element is given by

$$t_{\alpha}(\mathbf{r}) = t \langle \chi(\mathbf{r}) | \chi(\mathbf{r} + c\mathbf{n}_k) \rangle$$

where t is the original transfer integral of the conduction electron. $t_{\alpha}(\mathbf{r})$ is in general a complex number, and can be written as $t_{\alpha}(\mathbf{r}) = |t_{\alpha}(\mathbf{r})| e^{i\alpha(\mathbf{r})}$. This phase factor $e^{i\alpha(\mathbf{r})}$ is analogous to the Peierls factor in the presence of the external magnetic field and hence we can regard $a_{\alpha}(\mathbf{r})$ as the vector potential of an effective electromagnetic field. Assuming the slowly varying spin configuration over the lattice constant c , we obtain $a_{\alpha}(\mathbf{r}) = -i \langle \chi(\mathbf{r}) | \partial_{\alpha} \chi(\mathbf{r}) \rangle = \frac{1}{2} \partial_{\alpha} \Phi (1 - \cos\Theta)$. From this expression, one can easily confirm that the emergent magnetic field b_z is related to the solid angle as

$$b_z = \frac{\partial a_x}{\partial x} - \frac{\partial a_y}{\partial y} = \frac{1}{2} \mathbf{n} \cdot \left(\frac{\partial \mathbf{n}}{\partial x} \times \frac{\partial \mathbf{n}}{\partial y} \right)$$

Therefore, the **total emergent magnetic flux associated with a skyrmion is $2\pi N_{\mathbf{k}}$** . These considerations can be easily generalized to the three-dimensional case and also to the **emergent electric field e_{α}** as

$$b_{\alpha} = \frac{1}{2} \epsilon^{\alpha\beta\gamma} \mathbf{n} \cdot (\partial_{\beta} \mathbf{n} \times \partial_{\gamma} \mathbf{n}) \quad (B4a)$$

$$e_{\alpha} = \mathbf{n} \cdot (\partial_{\alpha} \mathbf{n} \times \partial_{\beta} \mathbf{n}) \quad (B4b)$$

where $\partial_{\alpha} = \partial/\partial x_{\alpha}$, $\epsilon^{\alpha\beta\gamma}$ is the totally antisymmetric tensor in three dimensions, and the coupling to the conduction electrons is described by the Lagrangian

$$L_{\text{int}} = j_{\mu} a_{\mu} \quad (B5)$$

with j_{μ} being the density and current density of conduction electrons as in the case of the Maxwell electromagnetic field A_{μ} . Here μ is the space-time index.

We mention here that the well-known spin-transfer torque arises from equation (B5). Namely, the variation of a_{μ} with respect to \mathbf{n} is given by

$$\delta a_{\mu} = -\frac{1}{2} \delta \mathbf{n} \cdot (\mathbf{n} \times \partial_{\mu} \mathbf{n}) \quad (B6)$$

Combined with the variation of the Berry phase term ω as $\delta \omega = -\frac{1}{2} \delta \mathbf{n} \cdot (\mathbf{n} \times \partial_{\mu} \mathbf{n})$, equation (B6) leads to the equation of motion as

$$[\partial_t + (\mathbf{j} \cdot \nabla)] \mathbf{n}(\mathbf{r}, t) = \mathbf{0}$$

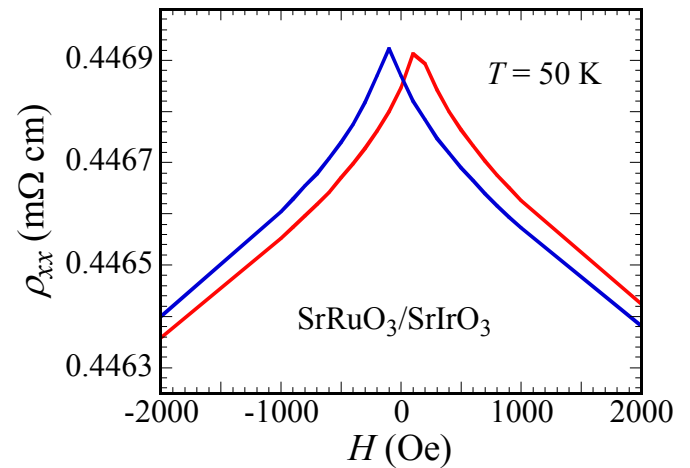
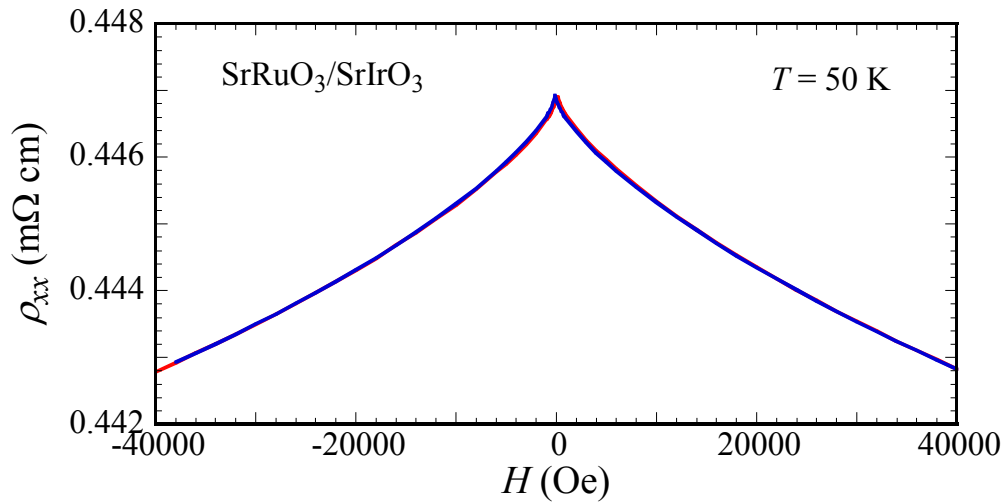
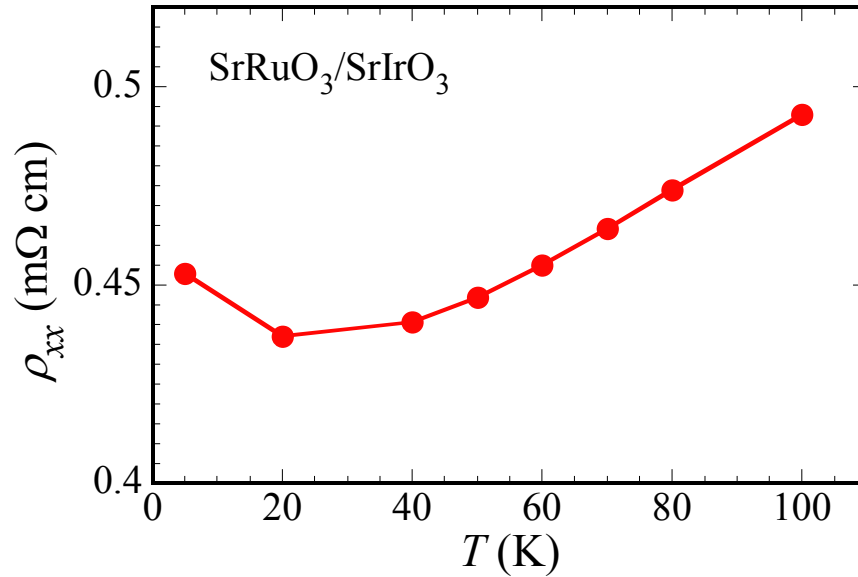
which describes the current-driven motion of the spin texture with spatially varying \mathbf{n} .

Skyrmions exhibit topological phenomena due to the **emergent electromagnetic field (EEMF)**

- The topological Hall effect is induced by the **emergent magnetic field** of the skyrmions on conduction electrons.
- The motion of the skyrmions leads to the **temporal change of the emergent magnetic field**
- An **electromagnetic induction**.
- The **induced emergent electric field** contributes to the Hall effect when the skyrmions move

Nagaosa & Tokura,
Nature Nano. 8, 899
(2013)

Longitudinal resistivity of SrRuO₃/SrIrO₃ bilayers



Topological Hall effect in skyrmion films

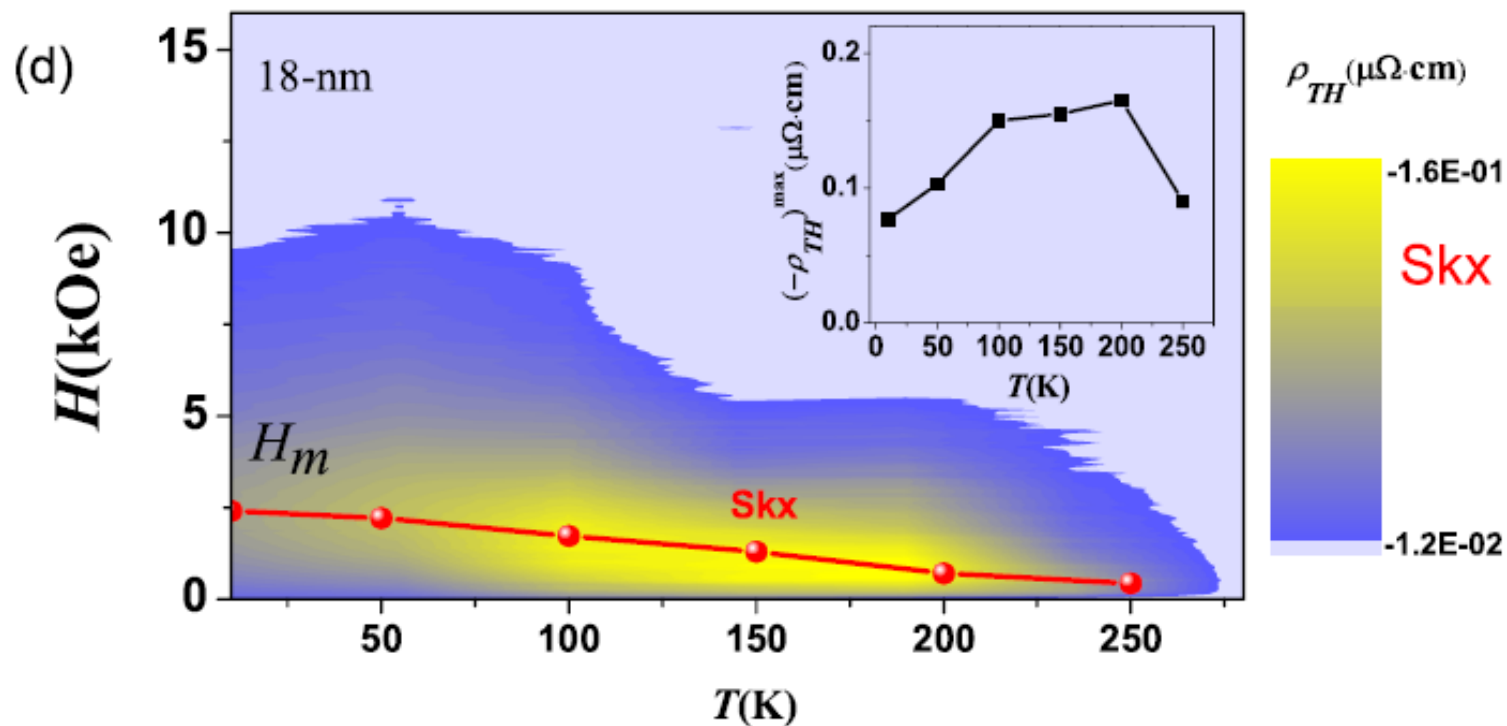
PRL 108, 267201 (2012)

PHYSICAL REVIEW LETTERS

week ending
29 JUNE 2012

Extended Skyrmion Phase in Epitaxial FeGe(111) Thin Films

S. X. Huang* and C. L. Chien†



Huang & Chien. *Phys. Rev. Lett.* 108, 267201 (2012)

Topological Hall effect in skyrmion films

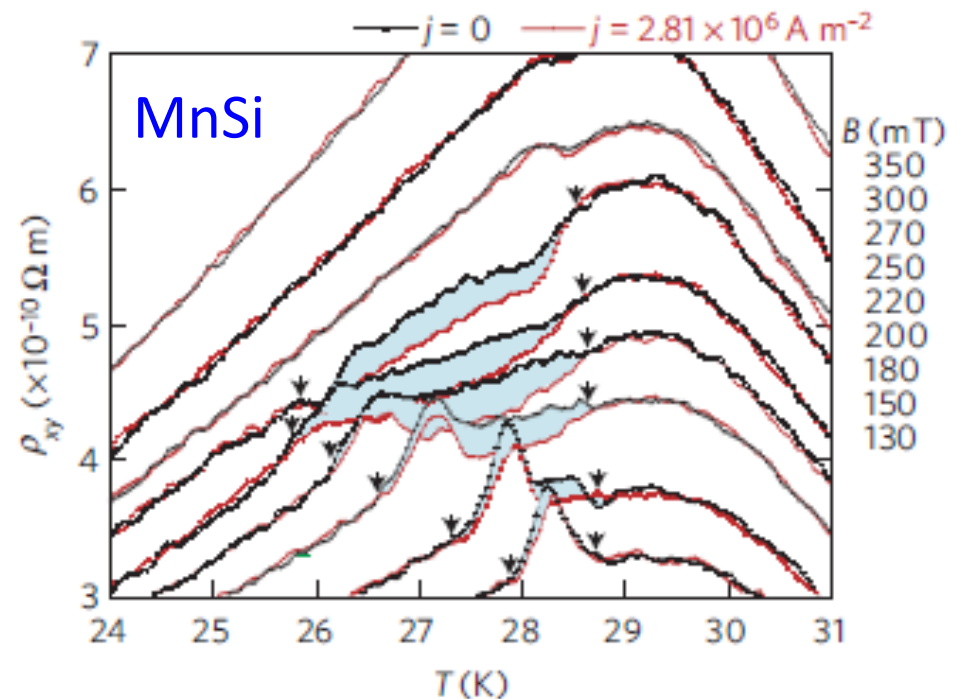
nature
physics

LETTERS

PUBLISHED ONLINE: 19 FEBRUARY 2012 | DOI: 10.1038/NPHYS2231

Emergent electrodynamics of skyrmions in a chiral magnet

T. Schulz¹, R. Ritz¹, A. Bauer¹, M. Halder¹, M. Wagner¹, C. Franz¹, C. Pfleiderer^{1*}, K. Everschor², M. Garst² and A. Rosch^{2*}



Schulz, et al. *Nat. Phys.* 8, 301 (2012)